Available online at www.jourcc.com

Journal homepage: www.JOURCC.com

Journal of Composites and Compounds

Application of different nanocatalysts in industrial effluent treatment: A review

Sara Eskandarinezhad [a] , Reza Khosravi [b], Mohamadamin Amarzadeh [c], Piyal Mondal [d], Fernando Jorge Correa Magalhães Filho [e]*

[a] *Department of Mining and Metallurgy, Yazd University, Yazd, Iran*
[b] *Department of Chemical Engineering, Faculty of Engineering, Ferdowsi University of Mashhad, Mashhad, Iran*
[c] *Department of Safety Engineering, Abadan Faculty of Petroleum Engineering, Petroleum University of Technology, Abadan, Iran*
[d] *Department of Chemical Engineering, Indian Institute of Technology Guwahati, Guwahati, 781039, India*
[e] *Departamento de Engenharia Sanitária e Ambiental, Universidade Católica Dom Bosco, Campo Grande, Brazil*

A B S T R A C T

The manufacturing, application, and design of chemical processes and products that minimize or remove waste and the use of dangerous and toxic reagents are referred to as green chemistry. Green chemistry is made up of twelve principles, one of which is catalysis. The role of catalysis is to accelerate the reaction by introducing a substance called a catalyst. Because of their high efficiency, productivity, activity, and selectivity, nanocatalysts have recently received many interests. Nanocatalysts are characterized by their high surface area to volume ratio, as well as their nanoscale forms and sizes. One of the significant applications of nanocatalysts is wastewater and wastewater purification. Green and bio-synthesized nanocatalysts could be used efficiently to remove heavy metals, medicinal, organic, and inorganic pollutants from the wastewater systems. This paper reviews nanocatalysts based on noble and magnetic nanocatalysts, as well as metal catalysts supported by organic polymers, and discusses their industrial effluent treatment mechanisms.

Peer review under responsibility of JCC Research Group

A R T I C L E I N F O R M A T I O N

Article history:
Received 15 December 2020
Received in revised form 24 February 2021
Accepted 20 March 2021

Keywords:
Green chemistry
Magnetic nanocatalyst
Noble nanocatalysts
Organic polymer-supported metal catalysts

Table of contents

1. Introduction

The rapid expansion of various manufacturing sectors has adverse effects on the environment, particularly on the aquatic one, since most industries have wastewater composed of organic and inorganic pollutants with high concentration. As an example, various industries, including textile, paint, pharmaceutical, printing, leather, paper, and carpet, have produced daily a large number of aromatic pollutants, including many types of nitro compounds and dye. These industries would release large quantities of residual pollutants even if they were refined using conventional techniques [1-5]. Biodegradation of most of these aromatic pollutants dissolved in water is very hard, therefore becoming a long-term and direct toxic threat to aquatic and amphibian lives, animals, and microorganisms. Finally, this process affects humans since the lives on land depend on aquatic products and water, and some of these pollutants are extremely toxic, mutagenic, and carcinogenic [5-7].

Anastas and Warner in 1998 [8] proposed twelve principles called the principles of green chemistry to eliminate and reduce chemical substances and processes that are harmful to the environment. Fabrication and development of catalysts is an essential principle of green chemistry. These principles state that catalytic reagents are better than stoichiometric reagents since catalytic reagents are applied in small quantities and carry out one reaction several times, but stoichiometric reagents are

* *Corresponding author: Sara Eskandarinezhad; E-mail: s.eskandari.nezhad@gmail.com*
DOR: 20.1001.1.26765837.2021.3.6.5.8
https://doi.org/10.52547/jcc.3.1.5

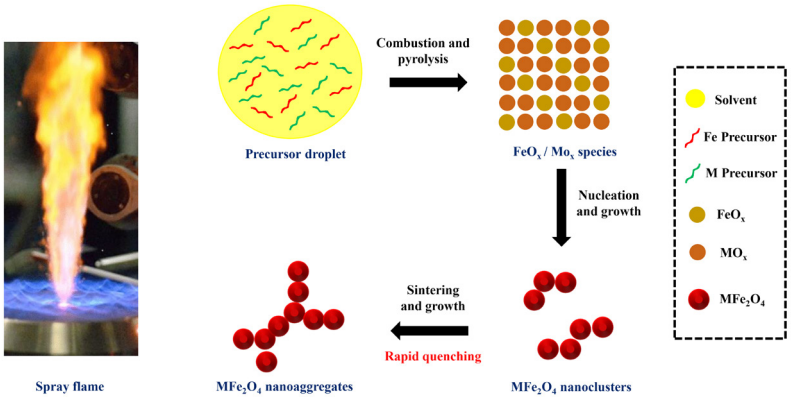

Fig. 1. Schematic illustration of the chainlike MFe_2O_4 nanoaggregates formation using spray flame.

applied further and work only once [9, 10]. The base of these twelve green chemistry principles is to work similarly to nature. If the catalyst is not used, humans' necessary products, such as lubricants, paints, fuels, fibers, polymers, fine chemicals, medicines, will not be produced. Catalysis is a process that helps chemical transformations take place, allowing for the industrial processing of required products [11, 12]. Therefore, applying catalyst fabrication methods can be rendered more sustainable, cost-effective, and environmentally friendly. Soft catalysts such as crown ethers (as phase transfer catalysts) and zeolites have more industrial applications than heavy metal catalysts, which are usually non-recoverable [13]. Enzymatic catalysis is the greenest and most effective catalysis in nature among three classifications of enzymatic, heterogeneous, and homogeneous catalysis. Heterogeneous and homogeneous catalysis has some advantages and limitations; therefore, it is crucial to create a novel catalytic mechanism that is easily recoverable and active, like heterogeneous and homogeneous catalysis, respectively [14].

Nanomaterials offer promising properties originating from their high surface area [15, 16]. Nanocatalysts have both advantages of the heterogeneous and homogeneous catalytic system [17, 18]. This system provides ease of catalyst recovery and separation as well as selective, and rapid chemical transformations with good product yield. One of the essential features of a catalyst is the ability to be recovered before being used in industry as green chemical manufacturing processes [19, 20]. One of the advantages of homogeneous catalysis is that the interaction between catalyst and reactants is significantly improved due to their nanosize and high surface area. Because of the catalyst's insolubility in the solvent, it is heterogeneous and hence it could be readily removed from the solution, which is one of the properties of heterogeneous catalysis [21]. Several authors have studied many magnetic [22-24], zinc [25, 26], cobalt [27, 28], and copper-based [29, 30] nanocatalysts. In this work, different nanocatalysts in industrial effluent treatment, including zinc-based nanocatalysts, cobalt-based nanocatalysts, copper-based nanocatalysts, and magnetic nanocatalysts, and their mechanism of action have been studied. Moreover, recent advancements have been reported.

2. Nanocatalysts

One of the first applications of nanoparticles is Catalysis. Several materials and elements such as silica, clays, titanium dioxide, iron, and aluminum have been applied as catalysts in nanoscale [31-35]. Nevertheless, there is no suitable explanation and the exact reason for nanoparticles' excellent catalytic behavior. The wide nanoparticles' surface area directly affects reaction rate and it can be a good reason for its catalytic performance [36]. The properties of structure, shape, and nanosize of any substance affect their catalytic performance. A better selectivity was achieved by well-adjusting nanocatalyst composition, including the use of supports, core-shell type, and bimetallic size and shape. By showing how the physical properties and preparation parameters associated with nanoparticles influence their catalytic characteristics, nanocatalysts with high activity, selectivity, and resilience can be designed. These advantages led to enabling industrial chemical reactions to produce less waste, consume less energy, and become more resource-efficient, reducing the environmental effect caused by applying chemical processes [37-39]. Nanoparticles are one of the most crucial catalysts for industrial purposes with many applications in chemical manufacturing, energy storage, and conversion. The heterogeneity and differences in shape and size of nanoparticles led to their special catalytic performance [40, 41].

According to the effect of nanomaterial intrinsic features on catalysis, the meaning and concept of nanocatalyst will be understood [42]. The intrinsic properties of nanomaterials that significantly affect the catalytic performance [21, 43] could be classified as follows: quantities directly connected with the bond length, including binding energy, atomic density, as well as mean lattice constant. Surface densification and relaxation are caused by lattice contraction in a nano solid.

Quantities that relied on the cohesive energy per atom, including diffusion, the activation energy for chemical reactions, atomic dislocation, evaporation in a nano solid, phase transitions, critical temperature, Coulomb blockade, thermal stability, and self-organization growth.

The Hamiltonian, which defines the whole band structure, as well as attributes like photoemission, core level energy, and bandgap differs by the binding energy density in the relaxed continuum zone.

Qualities that result from the combined influence of the density of binding energy and energy of atomic cohesiveness including the magnetic performance of a ferromagnetic nano-solid, compressibility of a nano-solid, extensibility, surface energy, surface stress, Young's modulus, and mechanical strength.

3. Application of various nanocatalysts in industrial effluent treatment

3.1. Nanocatalysts based on magnetic metals

Gawande et al. [14] investigated the application of surface-functionalized nano magnetite supported nanoparticles in pharmaceutically significant, green chemistry, and catalysis reactions. Magnetite-supported metal nanocatalysts have been effectively applied in organic synthesis for various crucial reactions and they act as the catalytically active site [44-46]. The most important examples of these catalysts are Ni, Co, and Ferrites metal alloys. Some researchers have applied spinel ferrites for

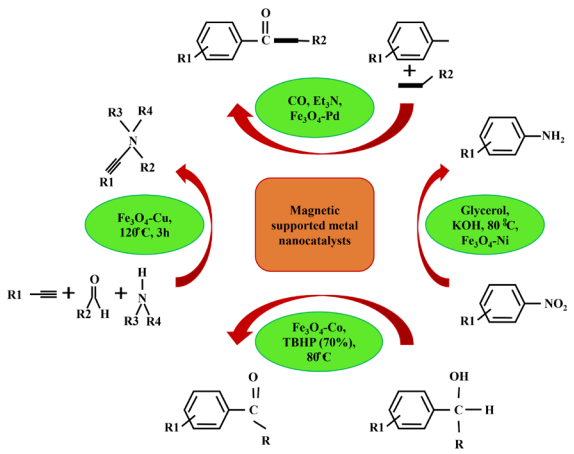

Fig. 2. Catalysis reactions of some organic components by metal nanoparticles supported by magnetite.

dyes and nitroarenes reduction. For example, Feng et al. [47] studied the $CuFe_2O_4$, which was prepared by hydrothermal technique; it has a high catalytic activity for nitrophenol reduction in the sodium borohydride presence. Li et al. [48] used the spray pyrolysis method to synthesize the chainlike spinel MFe2O4 (M = Cu, Ni, Co, and Zn). (Fig. 1). It was revealed that $CuFe_2O_4$ has the best catalytic performance for the nitroaromatic reduction compared to $ZnFe_2O_4$, $CoFe_2O_4$, and $NiFe_2O_4$.

Goyal et al. [49] have studied the catalytic efficiency of nano ferrites of MFe_2O_4 (M = Zn, Cu, Ni) as well as Mn-doped $CoFe_2O_4$ catalysts for the 4-NP catalytic reduction [50]. These samples were provided by the sol-gel process. $CuFe_2O_4$ presented higher catalytic performance between the synthesized ferrites while pure $CoFe_2O_4$ was not active, but the addition of Mn ions improved its catalytic efficiency. The synergistic effect of the Fe^{3+}, Mn^{3+}, and Co^{3+}, which were in the octahedral sites, could be accountable for improving catalytic activity. $CoMn_{0.2}Fe_{1.8}O_4$ showed the highest catalytic performance. Kiran et al. [51] studied the Bi^{2+} catalytic performance substituted nanoparticles of $CoFe_2O_4$, which were synthesized by co-precipitation and combustion methods, and revealed that the sample synthesized by combustion technique showed better catalytic activity in comparison with the nanoparticles synthesized using the co-precipitation technique. Singh et al. [52] synthesized Ni^{2+}-doped $CoFe_2O_4$ ($Ni_xCo_{1-x}Fe_2O_4$ nanoparticles by the reverse micelle method. Dey et al. [53] studied the cube-shaped magnetic $NiFe_2O_4$ nanoparticle for 4-nitrophenol (4-NP) catalytic reduction. Dhiman et al. [54] prepared several morphologies of $NiFe_2O_4$ hydrothermally using varying reaction conditions, solvents, additives, and precursors. It was reported that the catalytic performance of all the provided morphologies for reduction reactions depends on the surface area. The $NiFe_2O_4$ nano cord morphology showed the highest surface area and highest catalytic property. Papadas et al. [55] prepared three-dimensional mesoporous $BiFeO_3$ using a process of nanoparticle templating, which in the first step involved the synthesis of polymer-assisted aggregating formation of 3-aminopropanoic acid stabilized $BiFeO_3$ nanocrystals, accompanied by thermal decomposition to eliminate surfactant molecules . Catalysis reactions of some organic components by metal nanoparticles supported by magnetite are presented in Fig. 2.

Amir et al. [56] studied the degradation of organic dyes, including methylene blue (MB) and methyl orange (MO), using the recyclable magnetic nanocatalyst of Fe_3O_4@His@Ag in which histidine was applied as a linker. According to catalytic analysis, this nanocatalyst can lead to MB and MO degradation at the appropriate time. This material could also be recovered five times using magnetic separation while it maintains most of its activity. Kurtan et al. [57] prepared a magnetically recyclable nanocatalyst of $MnFe_2O_4$@SiO_2@Ag by chemical reduction and co-precipitation method. The reduction of several azo compounds, including rhodamine B (RhB), eosin Y (EY), MB, and MO, as well as aromatic nitro compounds like 4-NP and 2-nitroaniline (2-NA), 4-nitroaniline (4-NA), was catalyzed by a magnetically recyclable Mn-Fe_2O_4@SiO_2@Ag nanocatalyst. Furthermore, the magnetic nanocatalyst exhibits high recyclability, with qualities that are maintained after multiple using cycles. Mohammadi et al. [58] studied the *in situ* and green synthesis of Fe_3O_4@SiO_2Ag magnetic nanocatalysts employing safflower (Carthamus tinctorius L.) flower extract with no surfactants or stabilizers. For the reduction of MO, MB, and 4NP, the catalytic activity of the resulting nanocatalyst was investigated at room temperature. To reduce MB, MO, and 4NP, the noticeable rate constants were 0.09 s^{-1}, 0.064 $s^{-1,}$ and 0.756 min^{-1}, respectively. A magnet was used to recover the catalyst, which was then reused for multiple cycles without losing its function. Veisi et al. [59] studied the surface functionalization of Fe_3O_4 nanoparticles with thiol groups to immobilize Ag nanoparticles, resulting in Fe_3O_4/SiO_2-Pr-S-Ag nanoparticles. Fe_3O_4/SiO_2-Pr-S-Ag NPs have excellent catalytic efficiency as a reusable nanocatalyst for the MB, RhB, and 4-NP degradation in an aqueous solution at room temperature. Ghosh et al. [60] investigated a convenient procedure for the synthesis of a new nanocatalyst containing Ag, $CoFe_2O_4$, and mesoporous TiO_2 nanoparticles for three essential reactivities: (i) photocatalytic MB degradation, (ii) 4-NP reduction, and (iii) styrene epoxidation. The prepared catalyst showed a high catalytic performance to these three reactions. Within 10 hours, they recorded a 98 percent conversion of styrene and a 95 percent selectivity of styrene oxide. The result showed that this catalyst reduced 4-nitrophenol in 4 minutes with k_{app} = 1.08 min^{-1}. When exposed to visible light for 60 minutes, the catalyst exhibited total photodegradation of MB. In addition, the catalyst was readily restored using a permanent magnet externally as well as exhibited excellent reusability. Najafinejad et al. [61] prepared Au nanoparticles supported on Fe_3O_4@ polyaniline, and their activity in eliminating MB and MO from aqueous systems was investigated. Two nanocatalyst concentrations were applied at room temperature to examine the impact of nanocatalyst dosage on the degradation rate of azo dyes. When azo dyes are degraded with $NaBH_4$, the reaction is 10^3 to 10^4 times quicker than degrading without the nanocatalyst. A list of recent nanocatalysts based on magnetic metals for treating various industrial effluents is provided in Table. 1.

3.2. Nanocatalysts based on noble metals

The noble metals, such as Pt, Pd, Ag, and Au, make most catalysts for the reduction reaction, but their high cost has limited their practical applications [65-67]. Because metal-based catalysts can reduce their high surface energy, they can quickly aggregate with no effective protection or stabilization of the nanocatalysts, resulting in deterioration of their catalytic performance and decreased lifespan. [68-70]. For example, the aggregation of bimetallic NPs of Ag–Au occurs without protection by a surfactant of the triblock copolymer; at room temperature, the bimetallic NPs stabilized by surfactants can be stable for weeks [71, 72]. The results showed that Pd and Pt have excellent adsorption energy properties [73, 74]. The microwave-polyol process was used to create Pd, Pt, Pd@Ag, and Pt@Ag nanoparticles, and the nano boxes of these core/shell systems prepared by galvanic replacement reactions showed optical properties. [75, 76]. Besides, Gu et al. [77] reported the photochemical creation of Pd, Pt, and Ag monometallic NPs supported on graphene/ZnO and applied these multi-hybrid nano-architectures as electrocatalysts for H_2O_2. The free Ag NPs prepared by several various methods are also reported [78].

Salem et al. [79] prepared Pt@Ag and Pd@Ag core/shell nanoparticles using the citrate method in two steps (Fig. 3). To examine the catalytic performance of these nanostructures of core/shell, the Congo

Table 1.
Nanocatalysts based on magnetic metals for the degradation of pollutants in wastewater

Authors/Country	Nanocatalysts	Synthesis Methods	% removal/ reduction	Catalytic behaviors
Oliveira et al. [62] Brazil	TiO_2:$CoFe_2O_4$	$CoFe_2O_4$ via Combustion and TiO_2:$CoFe_2O_4$ via Pechini method	Degradation ~100% and efficient mineralization of diuron (DRN)	Reducing the concentration of $CoFe_2O_4$ improved the photocatalytic systems mineralization. The photocatalytic treatment decreased the toxicity of the system and amplified CE50 from 1.5% to 14%.
Mohamed et al. [63] Saudi Arabia	TiO_2/α-Fe_2O_3 nanocomposite	Co-precipitation	Degradation of MB~98%	TiO_2/α-Fe_2O_3 nanocomposites exhibited better photocatalytic performance compared to pure Fe_2O_3 or TiO_2 nanomaterials; increased α-Fe_2O_3 concentration enhanced the activity.
Feng et al. [47] China	$CoFe_2O_4$	Hydrothermal technique	Nitrophenol reduction~95%	Reduction happened in the presence of sodium borohydride.
Li et al. [48] China	Chainlike spinel MFe_2O_4 (M = Cu, Ni, Co, and Zn)	Spray pyrolysis method	Nitroaromatic reduction ~100%	$CoFe_2O_4$ has the best catalytic performance in reducing nitroaromatic compared to $ZnFe_2O_4$, $CoFe_2O_4$, and $NiFe_2O_4$
Goyal et al. [49] India	MFe_2O_4 nano ferrites (M = Zn, Cu, Ni), Mn-doped $CoFe_2O_4$	Sol-gel method	2-NP reduction~95%	Fe^{3+}, Mn^{3+}, and Co^{3+} enhanced the catalytic performance, $CoFe_2O_4$was the best ferrite catalyst, $CoMn_{0.2}Fe_{1.8}O_4$ was the best catalyst
Kiran et al. [51] India	Bi^{2+} substituted nanoparticles of $CoFe_2O_4$	Co-precipitation and combustion methods	4-NP to 4-AP reduction in 2.25 min	Combustion method results had better catalytic performance than co-precipitation process
Singh et al. [52] India	Ni^{2+}-doped $CoFe_2O_4$ ($Ni_xCo_{1-x}Fe_2O_4$) nanoparticles	Reverse micelle method	Reduction of 4-nitrophenol, degradation of Rhodamine B ~99%	Photo-oxidative degradation of Rhodamine B, $NaBH_4$ was used as the reducing agent.
Dey et al. [53] India	Cube-shaped magnetic $NiFe_2O_4$ nanoparticle	Novel method	4-nitrophenol (4-NP) catalytic reduction	Effective, reusable nickel ferrite magnetic nanocatalyst without implementing any functionalization,
Dhiman et al. [54] India	Several morphologies of $NiFe_2O_4$ hydrothermally	Varying reaction conditions, solvents, additives, and precursors	Degradation of anionic remazol brilliant yellow (RBY) ~90% and cationic safranine-O (SO)	$NiFe_2O_4$ nano cord morphology had the highest surface area and the best catalytic performance
Papadas et al. [55] USA	Three-dimensional mesoporous $BiFeO_3$	Nanoparticle templating	Reduction of p-nitrophenol to p-aminophenol with $NaBH_4$, ~98%	The MBFAs (kapp= 0.018 s^{-1}) reduction rate was two times quicker than arbitrary $BiFeO_3$ NP aggregates (0.009 s^{-1})
Amir et al. [56] Turkey	Fe_3O_4@His@Ag (histidine was applied as a linker)	Hydrothermal method	Complete degradation of MO and MB	Degradation of MB and MO at a reasonable time. Reusable five times.
Kurtan et al. [57] Turkey	$MnFe_2O_4$@SiO_2@Ag	Chemical reduction and co-precipitation method	Complete reduction of rhodamine B (RhB), eosin Y (EY), MB, MO. Reduction of 4-NP as well as 2-nitroaniline (2-NA), 4-nitroaniline (4-NA), and.	Remained unchanged after multiple uses
Mohammadi et al. [58] Iran	Magnetic nanocatalyst of Fe_3O_4@SiO_2-Ag	Green and in situ synthesis, prepared by safflower (Carthamus tinctorius L.) flower extract	Reduction of 4-NP, MO, and MB at ambient temperature ~98%	The apparent constant rate for MB, MO, and the 4-NP reduction was 0.09 s^{-1}, 0.064 s^{-1}, and 0.756 min^{-1}. Recoverable by the magnet and reusable.
Ghosh et al. [60] India	Nanoparticles of Ag, $CoFe_2O_4$, and mesoporous TiO_2	EDTA precursor-based method,	Complete photocatalytic degradation of MB, 4-NP reduction, styrene epoxidation ~98.1%	Reduction of 4-NP with kapp = 1.08 min^{-1} in 4 min, recoverable using magnet, reusable, and selectivity of styrene oxide.
Najafinejad et al. [61] Iran	Nanoparticles of Au supported on Fe_3O_4@ polyaniline	Reduction of Au^{3+} using a wild herbal extract (Allium Sp)	Reduce MB and MO from aqueous solutions	Degradation of azo dyes with $NaBH_4$ was 10^3 to 10^4 times quicker than degradation without employing the nanocatalyst.
Ranjith et al. [64] Taiwan	Hybrid rGO-TiO_2/Co_3O_4 nanocomposite	Co-precipitation	High reduction of MB and crystal violet dye	Compared to crystal violet dye, the decolorization of the MB dye was higher with reduced time. rGO/TiO_2/Co_3O catalyst could be applied to treat a variety of industrial dyes
Veisi et al. [59] Iran	Nanoparticles of Fe_3O_4/SiO_2-Pr-S-Ag. Fe_3O_4/SiO_2-Pr-S-Ag NPs	Surface modification of nanoparticles of Fe_3O_4 with thiol groups for the immobilization of Ag nanoparticles	Degradation of MB, RhB, and 4-NP high efficiently decolorized the dyes.	Significant catalytic performance with $NaBH_4$ in the water at ambient temperature, recyclable

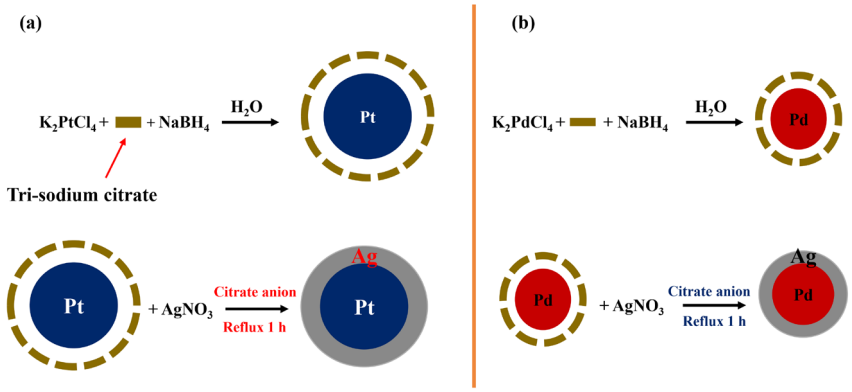

Fig. 3. Synthesis method of Pt@Ag and Pd@Ag core/shell.

red dye reductive degradation was selected. The electrons move from the reducing agent ($NaBH_4$) to the dye molecules through nanocatalysts, which serve as electron mediators. After four reaction cycles, the Pd@Ag nanocatalyst remained catalytically active. These results can be viewed as a cost-effective way to protect the environment by avoiding dye contamination in water supplies.

Moradi et al. [80] used the precipitation–decomposition method to create a range of Ag–ZnO/CNT nano photocatalysts with addition of multi-wall carbon nanotubes. The photocatalytic degradation of the Acid Orange 7 dye under visible light was used to determine the catalytic activity. As compared to the nanocomposite of Ag–ZnO and pure ZnO, the nano photocatalyst of Ag–ZnO/CNT with five wt. percent multi-wall carbon nanotubes loading had excellent photocatalytic activity. The efficient separation of pairs of electron hole on Ag–ZnO/CNT was related to improved photocatalytic performance. Duan et al. [81] synthesized the recyclable and high-performance nanocatalysts, which are composed of small, well-dispersed Ag nanoparticles that are immobilized on a Cu-based metal-organic substrate (MOF-199s) supported by CCFs (carboxymethylated cellulose fibers). The catalytic activity of AgNPs@MOF-199s/CCFs catalysts for the reduction of 4-nitrophenol to 4-aminophenol showed a high catalytic efficiency. Enhanced dispersion, the porous catalyst structures, and small particles of Ag stabilized by the MOF-199 s cause the high catalytic activity. Applying cellulose fiber led to the facilitation of the sustainability and reuse of nanohybrid catalysts revealing high and stable reusability of > 91% after five cycles.

Bao et al. [81] studied a one-pot method and used co-reduction growth in polyol mixture to synthesize amino-functionalized (-NH_2) graphene oxide (GO-) supported networked nanowires of Pd–Ag. The results showed effective catalytic activity with superior recovering efficiency at ambient temperature (25 ºC) for catalytic Cr(VI) reduction using the H_2 source of formic acid. The electron transfer from amino and Ag to Pd enhances Pd electron density, which improves the decomposition of formic acid and the reduction of Cr(VI). The catalytic reduction rate constant of Pd_3Ag_1/GO-NH_2 is 0.0768 min^{-1}, showing higher value compared to the monometallic Pd_3Ag_1/GO and Pd/GO-NH_2 catalytic reduction rate constants. Iqbal et al. [82] created a new form of recyclable, ecologically safe, and convenient cerium-doped magnesium-aluminum-layered double hydroxide (MgAl-LDH) nanocatalyst, known as MgAlCe-LDH@Au. It was fabricated by adding Au nanoparticles with an approximate diameter of 3 nm on MgAlCe-LDH support by *in situ* reductions of $HAuCl_4$ utilizing $NaBH_4$. This nanocatalyst shows very considerable activity in the 4-nitrophenol reductive degradation by $NaBH_4$ with k_{app} = 0.041 s^{-1} (rate constant) and TOF= 1.2 × 10^6 h^{-1} (catalyst turnover frequency); at ambient temperature (25 ºC) and air pressure, the reactions took place in an aqueous system. MgAlCe-LDH@Au nanocatalysts can be recovered and they can keep their original performance after seven catalytic processes. MgAlCe-LDH@Au is also an effective catalyst for the reductive breakdown of usual organic dyes, such as rhodamine 6G (R6G), rhodamine B, methylene blue, methyl orange, and Congo red that led to increased values of TOFs to 3.2 × 10^4 h^{-1}. Sahoo et al. [83] applied a simple one-pot production of trimetallic porous Au@Pd@Ru nanoparticles at ambient temperature. The trimetallic nanoparticles exhibited excellent catalytic performance in reducing p-nitrophenol and the breakdown of many azo dyes. The method was applied to eliminate color from wastewater using catalytic degradation of azo dyes.

Nasrollahzadeh et al. [84] used a structurally described furfural with a 3-aminopropyltriethoxysilane long tail to immobilize palladium nanoparticles on NH_2-modified zeolite (Zeo) particles carrying a heterocyclic ligand. At room temperature (25 ºC) in aqueous solutions, NH_2 modified Zeo/Pd was produced as a reusable, highly active, and sustainable nanocatalyst to reduce Nigrosin (NS), MB, RhB, 4-NP, 2,4-dinitrophenylhydrazine (2,4-DNPH), potassium hexacyanoferrate(III) ($K_3[Fe(CN)_6]$), and Cr(VI). UV–Vis spectroscopy was used to evaluate the rate of removal of these toxicants with NH_2 modified nanocatalyst of Zeo/Pd using formic acid (HCOOH) and sodium borohydride ($NaBH_4$) at ambient temperature (25 ºC), as well as the nanocatalyst's ability to be recovered eight times without remarkable reduction of catalytic performance. Yan et al. [85] used the one-pot solvothermal method to make bimetallic Pt-rhodium alloyed (PtRh ANMPs) nanomultipods in oleylamine (OAm), using co-structure-directing agents of cetyltrimethylammonium chloride (CTAC) and creatinine. The prepared nanocatalyst showed remarkable catalytic properties to reduce RhB and 4-NP by $NaBH_4$. In similar conditions, the prepared catalyst exhibited a highly facilitated TOF=1.0 × 10^{-3}/0.44 × 10^{-3} mol g^{-1} min^{-1} and k=0.209/0.354 min^{-1} for RhB and 4-NP reduction versus industrial Pt black. Table 2 shows a list of recent nanocatalysts based on noble metals for treating various industrial effluents.

3.3. Nanocatalysts based on organic polymer-supported metal catalysts

Because of their porous network structures and functionalities, polymer hydrogels were used as metal nanoparticle carrier systems [104]. They could be produced by several polymerization techniques, including polymerizations [105, 106], free-radical [107, 108], and ionic [109, 110] based on convenient and low-cost solution routes. As an example, a core-shell microgel containing a shell of cross-linked poly(N-isopropyl acrylamide) (PNIPA) and solid polystyrene (PS) core was applied to stabilize a nanocatalyst of Pd [111]. A spherical polyelectrolyte brush-based scheme with poly ((2-methylpropenoyloxyethyl) trimethylammonium chloride) long chains as a shell and a solid PS core was quantitatively contrasted to the microgel-based process [112]. The results

Table 2.
Nanocatalysts based on noble metals for the degradation of pollutants in wastewater

Authors/ Country	Nanocatalysts	Synthesis methods	% removal/ reduction	Catalytic behaviors
Katoch et al. [87] India	Bi_2O_3	Microflow	Degradation of MO ~96 %	Bi_2O_3 nanoparticles exhibited excellent stability after three cycles indicating coated microreactors in photocatalysis reusability.
Dang et al. [88] China	$CuCl_2$ nanoflake film grown on the top surface of nanoporous anodic alumina substrate (nano-PAA-$CuCl_2$)	Self-assembly approach	Degradation of MO~95% and MB~100%	Applicable in Fenton-like reaction as an effective process for wastewater treatment.
Rehman et al. [89] Saudi Arabia	Ce & Zn doped CuO nanocatalyst	Co-precipitation	Degradation of MO ~81%	The photocatalyst of binary metal-doped CuO exhibited excellent photocatalytic performance for the treatment of toxic industrial effluents.
Dehghan et al. [90] Iran	ZnO/rGO	Chemical deposition	Removal of Metalaxyl (MX) ~ 90%	The MX toxicity was dropped from 51 to 15 within 96 h. The photocatalytic performance was reduced by nitrate and phosphate ions but remained constant in the presence of other water anions.
Dosti et al. [91] Iran	Pd NPs	-	Reduction of Cr(VI) ~99% and Cr(III) precipitation ~96%	Electrochemical cells could perform in-situ total free chlorine production and chromium removal concurrently.
Shelar et al. [92] India	Ag-doped ZnO	Co-precipitation	Degradation of MB ~65-95%	The photocatalytic performance increase with the increase of concentration of dopant.
Ikram et al. [93] Pakistan	Ag decorated MoS_2 nano pedals	Adopting hydrothermal approach	Dye degradation in the presence of $NaBH_4$ ~100%	Excellent potential for removing hazardous toxins, including tannery pollutants and synthetic dyes, from industrial effluents.
Nasrollahzadeh et al. [94] Iran	Ag/MgO nanocomposite	-	Complete and excellent reduction of MB, 4-$NPMO_2$, and 4-DNPH ~100%	The Ag/MgO system was reusable, highly stable, with excellent catalytic performance.
Khoshnamvand et al. [95] China	Ag NPs	Green synthesis	Reduction of 4-NP, and antioxidant activity against DPPH, and ABTS+ ~99%	Ag nanoparticles exhibited excellent antioxidant activity against ABTS and DPPH free radicals and efficient catalytic performance in 4-NP reduction to 4-AP.
Kumar et al. [96] Ecuador	Ag NPs	Biosynthesis	Reduction of MB ~29% in 1 hour	Exhibited effective photocatalytic activity to remove MB dye (5 $mg.L^{-1}$, k = 0.00707788 min^{-1}).
Garol et al. [97] India	Pd NPs	Green synthesis	Complete reduction of 4-NP, MO, and MB	Excellent catalytic reduction performance for all organic contaminants; the occurrence of complete reduction in 10 min.
Salehi et al. [98] Iran	Pd/RGO NPs	Chemical deposition	Reduction of MB, MO, and rhodamine B ~99%	These nanoparticles have excellent catalytic reduction activity.
Khan et al. [99] Pakistan	ZnO-NPs	Green synthesis	Synozol Navy Blue-KBF textile dye degradation ~91%	Removed the dye in 159 min, potential to have various photocatalytic and biological applications.
Ganesh et al. [100] South Korea	ZnO Np	Green synthesis	Reduction MB ~96%	These green prepared nanoparticles of ZnO could be effective photocatalysts and anti-microbial for dye degradation and eliminating pathogenic microbes in industrial effluents.
Prasad et al. [101] India	ZnO NPs	Green synthetic strategy using Abelmoschus esculentus	Degradation MB~100%, Complete degradation of rhodamine B. Degradation of Congo red, and MO	ZnO nanoparticles are applied in selective photodegradation of the target cationic dyes.
Rajaendaran et al. [102] India	Ag-Mo/CuO NPs	Biogenic synthesis	Photodegradation of MB~99%	The photocatalytic performance by AzI-MACO (99%) was higher than that of AzI-MCO (88%), AzI-ACO (74%), AzI-CO (52%), and CO (39%) nanoparticles.

Table 2. (Continued)

Authors/ Country	Nanocatalysts	Synthesis methods	% removal/ reduction	Catalytic behaviors
Salem et al. [79] Egypt	Pt@Ag and Pd@Ag core/shell	Citrate method in two steps	Congo red dye reductive degradation ~85%	NaBH4 was used as a reducing agent; nanocatalyst was catalytically stable after four cycles
Moradi et al. [80] Iran	Ag–ZnO/CNT	Method of precipitation–decomposition	Acid Orange 7 dye photocatalytic degradation under visible light ~100%	Improved photocatalytic activity due to effective separation of pairs of electron-hole on Ag–ZnO/CNT compared to the nanocomposite of Ag–ZnO and the pure ZnO reusable
Iqbal et al. [83] China	MgAlCe-LDH@Au	Au nanoparticles loading on MgAlCe-LDH by an in situ reductions of $HAuCl_4$	Degradation of 4-nitrophenol ~100%, Complete degradation of rhodamine 6G (R6G), RhB, Congo red, MO, and MB	The reactions were in an aqueous system at room temperature and atmospheric pressure, reusable for seven cycles,
Sahoo et al. [84] India	Trimetallic porous nanoparticles of Au@Pd@Ru	Facile ambient temperature one-pot synthesis	Efficient p-nitrophenol reduction and degradation of reactive black (RB-5) and reactive red (RR-120)	Color removal and elimination of produced amine from wastewater
Nasrollahzadeh et al. [85] Iran	Pd NPs@Zeo	Immobilization of structurally defined furfural with 3-aminopropyltriethoxysilane long tail, multi-step organic amine functionalization	Reduction of Nigrosin (NS), MB, RhB, 4-NP, 2,4-dinitrophenylhydrazine (2,4-DNPH), potassium hexacyanoferrate (III) Cr(VI) and (K3[Fe(CN)6]),	Highly active, recoverable, and reusable for eight times at room temperature, antibacterial activity against E. coli.
Yan et al. [86] China	Nanomultipods of bimetallic PtRh-ANMPs in OAM by adopting the co-structure-directing agents of cetyltrimethylammonium chloride (CTAC) and creatinine	A facile one-pot solvothermal method	RhB ~97% and 4-NP ~94% reduction by NaBH4	Highly effective for RhB and 4-NP reduction than commercial Pt black under similar conditions, recyclable
Mohammadi et al. [103] Iran	Fe_3O_4/SBA-16-Cit-Cya-Au nanocomposite	Chemical deposition	Reduction of MB and MO, the reaction mixture turned colorless.	Sustainable and highly efficient after eight cycles.
Memar et al. [104] Iran	CuO/CuZnO	Chemical deposition	Degradation of MO and MB	Excellent catalytic activity and high repeatability after the fifth cycle of degradation reaction.

showed that the polyelectrolyte brush-based catalyst had better catalytic efficiency than the one stabilized by microgel, which may be linked with the various diffusional barriers present in such stabilizing processes. A bottlebrush polymer tightly linked on a solid core of PS was also investigated as an Ag nanoparticle carrier platform. However, the synthesis method is complicated, which can lead to high costs and difficulties in raw materials personnel, and time, restricting broad realistic implementations [113, 114].

Using electrostatic attraction, a microgel of polymethacrylic acid was applied as a carrier device to accumulate the metal ions, which were then reduced to the resulting metal nanoparticles [115]. Moreover, a modified cryogel of poly(4-vinyl pyridine) was applied to adsorb metal ions and reduction treatment for the production of a compound catalyst for 4NP and MB dye reduction [116]. Besides, amidodiol was used as a reducing agent and a cross-linking agent to adsorb Ag nanoparticles in a poly(acrylic acid)–based hydrogel fibrillar system [117]. The cationic dyes such as crystal violet, MB, and R6G were catalytically reduced with the synthesized hydrogel immobilized Ag nanoparticles. Temperature and pH were observed to have a remarkable influence on the catalyzed process. To prepare the Au and Ag nanoparticles, gel beads of calcium alginate (CA) were applied as stabilizing and reducing agents [118]. The researchers hypothesized that metallic Ag might be a superior catalyst compared to Au throughout this catalytic reduction process because the as-synthesized CA-stabilized nanocatalyst of Ag has been more effective for transforming of 4NP to 4AP compared to the Au equivalent. Also, the volume of Ag nanoparticles loaded on alginate or the surface covering with Ag nanoparticles was assumed to be more desirable for the catalyzed process than Au nanoparticles [109].

Metal catalysts could also benefit from the use of polymer dendrimers as stabilization systems. As an example, poly (amidoamine) (PAMAM) and poly (propylene imine) (PPI) dendrimers were applied to stabilize nanoparticles of Au for the reduction of 4NP [119, 120]. The results showed that as the dendrimer concentration increased, the rate constants of catalytic reduction for all of the processes studied declined. PPI and PAMAM dendrimers with amino groups on their surfaces were analyzed for synthesis and stabilization of Au compound nanocatalysts via laser irradiation reduction rather than chemical reduction [121]. With increasing the irradiation time, the mean size of the Au nanoparticles declined. According to the previous report, the dendrimers were adsorbed on the surfaces of NPs as a monolayer, lowering the efficiency of the catalytic performance. Furthermore, a layer-by-layer nanoreactor film was fabricated for holding silver nanoparticles utilizing a PAMAM dendrimer with positive charge and negatively charged polyacrylic acid or polystyrene sulfonate [122].

Polyacrylonitrile (PAN) substrate was also applied to embed silver nanoparticles by immobilizing the Ag nanoparticles within the polymer matrix. However, because of the blocking influence of the polymer matrix, nanoparticles of PAN/Ag matrix are inappropriate for catalytic applications. In addition, Ag nanoparticles were applied to the PAN nanofiber surface to expose most of their surface [123]. The nanofiber of PAN had been pre-modified for binding site incorporation before applying Ag nanoparticles upon its surface. Hydroxylamine hydrochloride

Table 3.
Nanocatalysts based on organic polymer-supported metal catalysts for the degradation of pollutants in wastewater

Authors/Country	Nanocatalysts	Synthesis method	Application: % removal/ reduction	Catalytic behavior
Kaliraji et al. [131] Korea	ZnO nano-flowers	Green synthesis	Removal of Eosin Y (EY), Malachite green (MG), and MB ~99%	High efficiency and reusability after five cycles without any remarkable loss in degradation performance.
Duan et al. [81] China	AgNPs@MOF-199s/ CCFs	Ag nanoparticles immobilized on a Cu-based metal-organic framework (MOF-199s) supported by CCFs (carboxymethylated cellulose fibers)	The 4-nitrophenol reduction to 4-aminophenol ~95%	Better dispersion improved the catalytic activity; cellulose fiber increased sustainability and reusability of >91% after five cycles.
M. Ajmal et al. [116] Saudi Arabia	A microgel of polymethacrylic acid	Inverse suspension polymerization	Absorb and reduce metal ions ~100%	A carrier system that uses electrostatic interactions to adsorb metal ions and then reduces the adsorbed metal ions to metal nanoparticles
Bhat et al. [129] Malaysia	The Pd catalyst based on the framework of chitosan-tannin (CT)	Glutaraldehyde chitosan crosslinking	The reduction of Congo red~23% and nitrate~71% in the absence and presence of H2.	Catalyst is considerably thermally-stable compared to CT support
Samai et al. [130] India	Nanocomposite of polyaniline/cerium oxide	Hydrothermal method.	The removal of RhB~91% in wastewater under irradiation of the UV light.	Polyaniline polymer was employed as active catalyst support to enhance the cerium oxide nanoparticle photocatalytic activity.
Nasrollahzadeh et al. [132] Iran	Pd/reduced graphene oxide (RGO) nanocomposite	Chemical deposition	Degradation of Cr(VI), 4-NP, CR, MB, and MO, the disappearance of absorbance peaks	Reusability and recyclability after multiple employment with no alteration in catalytic performance.
Peng et al. [133] China	Pd truncated octahedrons (PdTOs) and Pd NPs	Biosynthesis	Excellent reduction of 4-NP	The apparent rate constant (Ka) over PdTOs was 0.358 min^{-1} in p-NP reduction, which is improved compared to spherical PdNPs-0 (0.08 min^{-1}).
Gu et al. [77] China	Pd, Pt, and Ag monometallic NPs supported on graphene/ZnO	Photochemical synthesis	Electrocatalysts for H_2O_2	Distinct electrocatalytic activity
Bao et al. [82]ÿ China	Pd3Ag1/GO-NH_2	One-pot method	Excellent catalytic reduction of Cr(VI)	Formic acid (a H2 source) at room temperature, reduction rate constant was higher compared to the monometallic Pd_3Ag1/GO and Pd/GO-NH_2.
Sahiner et al. [117] Saudi Arabia	Modifiable Poly(4-vinylpyridine) (p(4-VP)) cryogels	Cryogellation using free radical polymerization method	Complete degradation of MB dye and reduction of 4NP	The cryogel embedded with Fe, Cu, Ni, and Co nanoparticles employed in an aqueous solution with $NaBH_4$
Narayanan [118] India	Polyacrylic acid–amidodiol hydrogels (SPAGs) entrapped Ag nanoparticle	Acrylic acid in situ polymerization and silver nitrate reduction utilizing amidodiol as cross-linking agent	Complete reduction of crystal violet, MB, and R6G	Temperature and pH had a remarkable influence on the catalytic reaction, easy separation, promising reusability, and absence of induction period.

has been utilized as a modifier by reacting with the –CN groups existing in PAN to create numerous amine as well as hydroxyl groups that could chelate Ag ions and immobilize them. Reduction treatment was used to build the Ag-decorated catalyst on the modified PAN fiber. A poly-(3,4) ethylene dioxythiophene (PEDOT) substrate was also used as a support base for Pd nanoparticles. [124]. The sodium polystyrene sulfonate (Na–PSS) catalytic reduction of the PEDOT supported nanoparticles of Pd in the solution was employed to improve the distribution of the PEDOT supported nanoparticles of Pd. The destructive impact on the catalyzed process must be considered because the surfactant Na-PSS is inclined to position the Pd catalyst. To stabilize Au and Fe_3O_4 nanoparticles, the conducting polymer polypyrrole (PPy) was utilized [125]. However, these nanoparticles were wrapped or embedded in a polymer substrate, creating a great diffusion barrier to the catalyst impairing MB dye catalytic activity. The carrier platform for the Au nanocatalyst [126] was Poly(allylamine hydrochloride) which was modified with composite sub microspheres poly(glycidyl methacrylate). The results showed that the carrier system's positive charges and epoxy groups could improve the catalyzed process. Epoxy groups have a role as electron acceptors because of their electrophilicity; therefore, they capture electrons and create an electron-rich region at the Au nanoparticle-sphere interface. This area could represent an electron reservoir, allowing the electron to be transferred to the reactant 4-NP in catalytic reduction of 4-NP; in the meantime, 4-NP anions could be adsorbed onto the positively charged surfaces of the sphere with ionic attraction. Aside from the multistep procedures and complex preparing requirements that restrict wide implementations, the composite sphere catalyst's reusability and stability have not been studied. Furthermore, the electrons captured by epoxy groups may not be freed, and the reduction of the epoxy groups could occur in the catalyzed reduction process by the captured electrons [1].

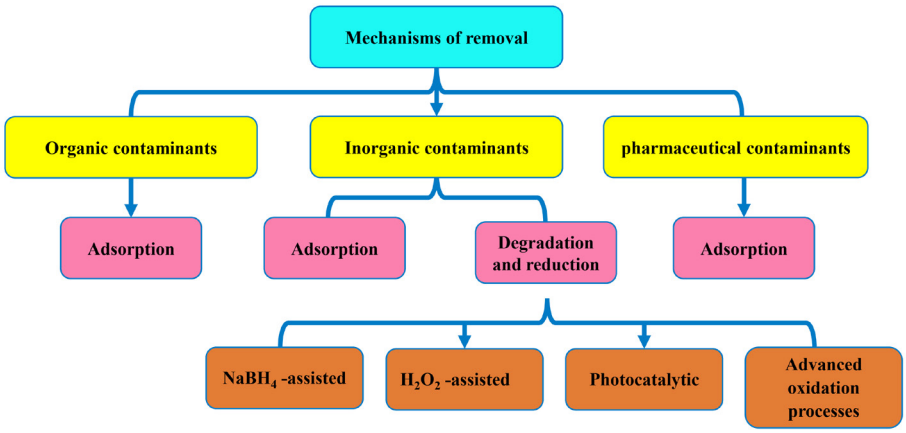

Fig. 4. Removal mechanisms by nanomaterials for different pollutants.

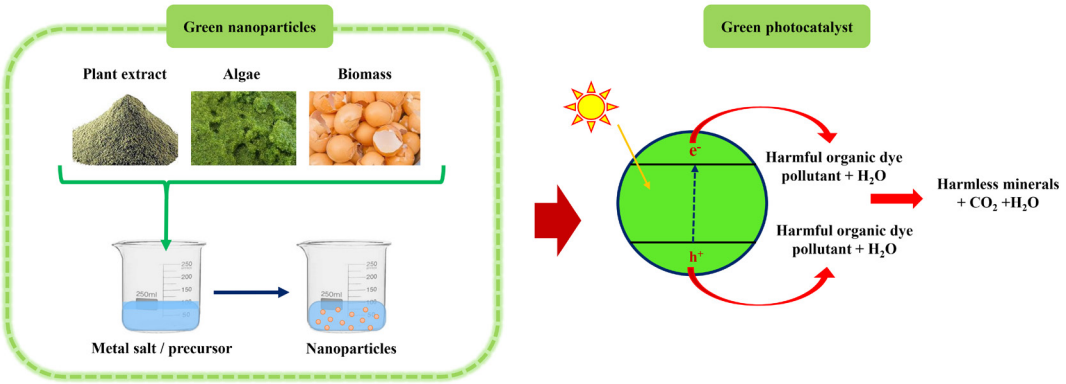

Fig. 5. Mechanism of dye photocatalytic degradation via green-synthesized nanoparticles.

To stabilize Au nanoparticles for the 4-NP reduction catalysis, quaternary ammonium resin beads of PS were used. The results showed that the tinier the Au nanoparticles, the quicker the catalyzed process. The Au nanoparticles immobilized on the surface of resin seem fragile because they could be dissociated with cationic surfactants, suggesting the composite catalyst's low endurance [127]. Bhat et al. [128] synthesized a Pd catalyst established on the chitosan-tannin (CT) framework. The catalyst's catalytic efficiency was investigated in the presence and absence of H_2 to reduce Congo red and nitrate. Within 60 and 20 minutes, respectively, the catalytic performances eliminated 23 percent and 71 percent of Congo red and nitrate.

Samai et al. [129] used a conducting polymer of polyaniline as active catalyst support to promote the cerium oxide nanoparticle photocatalytic activity. The as-prepared nanocomposite of polyaniline/cerium oxide shows significantly improved photocatalytic efficiency than some oxide nanoparticles or polyaniline for removing RhB in wastewater under the UV light irradiation. The results indicated that a nanocomposite containing cerium oxide nanoparticles and polyaniline in a 1:1 molar ratio degraded 91 percent of Rhodamine B in 2 hours, while cerium oxide nanoparticles only degraded 10%. Recent studies on applying various organic polymer-supported metal nanocatalysts for pollutant removal from wastewater are summarized in Table 3.

4. Catalytic mechanisms

Different types of biological, chemical, and physical technologies such as advanced oxidation processes (AOPs), ultra-filtration, membrane, sedimentation, flocculation, adsorption, oxidation, reverse osmosis, and ion-exchange are employed for treating wastewater. Because of their excellent performance, good reproducibility, convenience, and ease of handling, AOPs including photocatalysis, Fenton reaction, ozonation, or their variations are used to remove organic contaminants [134].

AOP is classified as remarkably nonselective and reactive chemical oxidants, including $\bullet O_2$, O_3, H_2O_2, and •OH to remove resistant and non-biodegradable organic pollutants.

As shown below, the Fenton reaction by radical of •OH is a low-cost, efficient, and sustainable wastewater treatment process. [135]:

$Fe^{2+} + H_2O_2 + H^+ \rightarrow Fe^{3+} + \bullet OH + H_2O$

Jaafar et al. [136] have studied some quantum calculations based on the ELF (electron localization function) and DFT (density functional theory) to investigate the removal process of Neutral Red dye (NR) in sewerage. In an aqueous medium, the Fenton reaction mechanism between free radicals (•OH) and the NR dye for its degradation was examined. For eliminating organic and inorganic pollutants and eradication of toxins (Fig. 4) from wastewater, freshwater sediments, groundwater, and other sites, a variety of pathways have been used, including reduction and (photo)degradation, adsorption, and UV photolysis/photocatalysis [137].

Nanomaterials can adsorb or degrade the contaminants using several catalytic approaches, including photocatalysis, H_2O_2, and $NaBH_4$, whereas green-synthesized nanoparticles are an excellent choice for photocatalytic wastewater treatment (Fig. 5) [138]. Toxic organic pollutants are broken down into other materials [139] or fully mineralized components, producing water, carbon dioxide, or other inorganic ions. In general, a semiconductor such as TiO_2 is capable of absorbing light with a wavelength equal to or greater than the wavelength of the semi-

conductor bandgap, resulting in the creation of electron-hole (e^--h^+) pairs [140, 141]. Reduction-oxidation reactions involve the interaction of nanocatalyst with adsorbate molecules. As shown in the equations below, h^+_{vb} interacts with surface-bound water to form •OH, and oxygen selects e-CB to form a superoxide radical anion..

New green prepared metal-organic framework-based photocatalytic materials have recently received a great deal of interest, particularly because of their capacity for environmentally friendly removal of toxic organic contaminants. [142-144]. Several studies have reported on the use of transition metals in MOF-based photocatalysts to remove extremely toxic contaminants under UV/vis, UV, and visible light. First, a MOF-5 was utilized to act as an efficient photocatalyst [145, 146]; these MOFs have a wide absorption band in the 500-840 nm range, which is related to the delocalized electron that lives on a time scale of microsecond and is most probably occupies a conduction band, with a value of conduction band energy equal to 0.2 V vs. NHE and a 3.4 eV bandgap. For the degradation of aqueous phenol, this method showed proportional performance with TiO_2 or ZnO. MOF-5 is an efficient photocatalyst since it is in a charge-separated state, with holes in the valence bands and electrons in the conduction band. As a result, phenol photodegradation can be accomplished by a series of reactions, including the primary formation of radical cations through transferring a phenol electron to the MOF-5 hole, or the oxygen active specie formation, including superoxide radical anions, by the interaction between photo-ejected electrons and oxygen. [147, 148]. Das et al. [149] prepared a double interpenetrated porous MOF (UTSA-38) containing Zn_4O with a bandgap of 2.85 eV, and its photocatalytic performance for the removal of MO in aqueous systems under UV/vis, visible light, as well as dark conditions was shown to be strong. According to the findings, under UV light for 120 minutes, methyl orange could be decayed into colorless smaller particles.

In reducing poisonous nitro compounds to useful and valuable amino compounds in aqueous systems, $NaBH_4$ has attracted much attention as a preferred alternative to hydrogen sources and a water-soluble reductant. Because metal hydride structures formed from BH_4-ions through π-π stacking interaction have been evaluated as intermediates in this reduction reaction, the activation of $NaBH_4$ is a major procedure that needs to take a metal material as the active site. The existence of a nanocatalyst of Pd stabilized amine-modified zeolite (Pd NPs@Zeo) with stacking interactions of π-π was found to explain the reduction of toxic 4-NP by $NaBH_4$ reductant [84]. Pd NPs@Zeo transform $NaBH_4$ to molecular H_2 and BO_2 dissociated on the nanocatalyst's surface, and the adsorbed 4-NP interacts with the dissociated H_2 gas to produce 4-aminophenol. Consequently, the as-synthesized aminophenol is eventually desorbed from the nanocatalyst base, resuming the catalytic process. The nanocatalyst also plays a part in facilitating simple reduction by adsorbing molecular H_2 or 4-NP nearby. Magnetically separable nano-bio hybrid catalysts, Fe_3O_4@Ch-PdNPs and Fe_3O_4@Ch-AuNPs, have been prepared and designed by a three-step procedure according to the process of biosynthetic mineralization [150]. Shewanella algae produced spherical Fe_3O_4 nanoparticles (35 nm) that were then coated or functionalized with chitosan, accompanied by modification with nanoparticles of Pd or Au to produce a reusable and water-dispersible nano-bio hybrid catalyst that showed significant functionality for 4-NP reduction and dye photodegradation (>99 percent) in contaminated water at ambient temperatures (25 ºC) [151].

This reaction was triggered by the adsorbent and reduction of methylene blue by Au or Pd nanoparticles via the electron transfer process. The reaction rates exhibited pseudo-second-order rate kinetics; under UV light, the Fe_3O_4@Ch-Pd and Au nanoparticles finished the methylene blue reduction in just 1 minute, with apparent rate constants (k_{app}) of 5.0 min^{-1} and 4.0 min^{-1}, respectively. Furthermore, the normalized rate constant (k_{nor}) values of the nanoparticles of Au and Fe_3O_4@Ch-Pd for the degradation of methylene blue are 1.14×10^2 and 1.72×10^2 $mmol^{-1}s^{-1}$, respectively, showing catalytic activities of the nanoparticles of Au and Fe_3O_4@Ch-Pd. For eliminating severely carcinogenic and toxic arsenic (As), green-fabricated amorphous nanoparticles of Fe with 51 m^2 g^{-1} Brunauer–Emmett–Teller (BET) area were employed [150].

Arsenate was reported to be evenly adsorbed on the surfaces of Fe nanoparticles; Fourier-transform infrared spectroscopy (FTIR) spectrometer analysis revealed that the adsorption was mainly due to a FeO-As bond, but X-ray photoelectron spectroscopy (XPS) findings show that only As(V) was adsorbed. Therefore, this method for eliminating arsenate relies on Fe nanoparticles interacting with arsenate to generate a monodentate chelating ligand, and then followed by a complex of bidentate binuclear. More studies showed that the synthesized nanoparticles' maximum arsenate adsorbent potential was about 14.6 mg g^{-1} and that the optimum range of pH for anionic arsenate adsorbent was around 4 to 6. [150]. The Langmuir adsorption isotherms showed that adsorption of As(V) by Fe nanoparticles matched their regression coefficient (R^2 = 0.99), confirming the suggested chemisorption; the adsorption yield matched the pseudo-second-order kinetic model favorably. As a result, the green synthesis of Fe nanoparticles is a promising option for removing arsenic while also being simple to synthesize.

5. Conclusions and future insights

This work focuses on organic polymer-supported metal catalysts, noble metals nanocatalysts, and magnetic nanocatalysts and then summarizes their mechanism in treating industrial effluent. Studies show the efficacy and promising application of these nanocatalysts for the removal of industrial effluents. Since low-cost preparation is critical for their uses in wastewater treatment, future research could focus on measurement of interactive mechanisms in the water treatment system of these nanomaterials and refining their economic viability. In addition, the toxicity of these nanomaterials for the environment and human health should be examined and (quali-quantitative) risk assessment evaluations are suggested in this regard. To ensure that their implementation is safe, general assessments of their harm are needed. More studies are required to compare the nanomaterials' relative performances to recognize favorable earth-abundant materials, resource utilization, and energy usage.

Some essential future perspectives should be considered for biogenic nanomaterials deployment for water purification and treatment. Comprehensive research is needed before these green-synthesized nanomaterials and nanocatalysts can be used on a commercial or industrial scale. Since these nanomaterials may result in secondary contamination, this critical problem must be thoroughly investigated. While the preparation of these nanomaterials is eco-friendly and simple, some challenging and essential factors, such as stability issues and the influence of reaction parameters, should be optimized and analyzed, as these factors can improve their pollutant removal activity, morphologies, and behavior of nanomaterials. Moreover, the extraction and purification of the synthesized biogenic nanomaterials are essential for additional applications. They should also be isolated as pure as possible for wastewater treatment. More studies are needed to find nanomaterials of multifunctional and innovative nanohybrids to improve their efficient utility. The cost-effectiveness of green-synthesized nanomaterials versus nanoparticles synthesized using traditional methods should be investigated. The assessment of restorative quality and efficacy issues is conducted in laboratory settings, simulating the parameter ranges of actual environmental levels, but it's vital to examine and analyze the outcomes from real-world scenarios.

Acknowledgments

The authors received no financial support for the research, authorship and/or publication of this article.

Conflict of interest

The authors declare that there is no conflict of interest that would prejudice the impartiality of this scientific work.

REFERENCES

[1] H. Hu, J.H. Xin, H. Hu, X. Wang, D. Miao, Y. Liu, Synthesis and stabilization of metal nanocatalysts for reduction reactions–a review, Journal of materials chemistry A 3(21) (2015) 11157-11182.
[2] M. Kamranifar, T.J. Al-Musawi, M. Amarzadeh, A. Hosseinzadeh, N. Nasseh, M. Qutob, F.S. Arghavan, Quick adsorption followed by lengthy photodegradation using $FeNi_3$@SiO_2@ZnO: A promising method for complete removal of penicillin G from wastewater, Journal of Water Process Engineering 40 (2021) 101940.
[3] A. Tkaczyk, K. Mitrowska, A. Posyniak, Synthetic organic dyes as contaminants of the aquatic environment and their implications for ecosystems: a review, Science of The Total Environment 717 (2020) 137222.
[4] C.G. Awuchi, H. Twinomuhwezi, C.G. Awuchi, V.S. Igwe, I.O. Amagwula, Industrial Waste Management, Treatment, and Health Issues: Wastewater, Solid, and Electronic Wastes, European Academic Research 8(2) (2020) 1081-1119.
[5] M. de Oliveira, B.E.F. Frihling, J. Velasques, F.J.C. Magalhães Filho, P.S. Cavalheri, L. Migliolo, Pharmaceuticals residues and xenobiotics contaminants: occurrence, analytical techniques and sustainable alternatives for wastewater treatment, Science of The Total Environment 705(0) (2020) 135568.
[6] B.K. Ghosh, S. Hazra, B. Naik, N.N. Ghosh, Preparation of Cu nanoparticle loaded SBA-15 and their excellent catalytic activity in reduction of variety of dyes, Powder Technology 269(0) (2015) 371-378.
[7] D. Kim, H. Kim, J.Y. Chang, Designing internal hierarchical porous networks in polymer monoliths that exhibit rapid removal and photocatalytic degradation of aromatic pollutants, Small 16(22) (2020) 1907555.
[8] P.T. Anastas, J.C. Warner, "Principles of green chemistry," in Green chemistry: Theory and practice, Oxford University Press, New York, 1998, pp. 29-56.
[9] G.E. Crisenza, P. Melchiorre, Chemistry glows green with photoredox catalysis, Nature communications 11(1) (2020) 1-4.
[10] Y. Ren, Y. Ma, G. Min, W. Zhang, L. Lv, W. Zhang, A mini review of multifunctional ultrafiltration membranes for wastewater decontamination: Additional functions of adsorption and catalytic oxidation, Science of The Total Environment 762 (2021) 143083.
[11] T.-L. Chen, H. Kim, S.-Y. Pan, P.-C. Tseng, Y.-P. Lin, P.-C. Chiang, Implementation of green chemistry principles in circular economy system towards sustainable development goals: Challenges and perspectives, Science of the Total Environment 716 (2020) 136998.
[12] C.H.C. Zhou, J.N. Beltramini, Y.X. Fan, G.M. Lu, Chemoselective catalytic conversion of glycerol as a biorenewable source to valuable commodity chemicals, Chemical Society Reviews 37(3) (2008) 527-549.
[13] V. Polshettiwar, R.S. Varma, Green chemistry by nano-catalysis, Green Chemistry 12(5) (2010) 743-754.
[14] M.B. Gawande, P.S. Branco, R.S. Varma, Nano-magnetite (Fe_3O_4) as a support for recyclable catalysts in the development of sustainable methodologies, Chemical Society Reviews 42(8) (2013) 3371-3393.
[15] L. Bazli, A. Khavandi, M.A. Boutorabi, M. Karrabi, Morphology and viscoelastic behavior of silicone rubber/EPDM/Cloisite 15A nanocomposites based on Maxwell model, Iranian Polymer Journal 25(11) (2016) 907-918.
[16] L. Bazli, A. Khavandi, M.A. Boutorabi, M. Karrabi, Correlation between viscoelastic behavior and morphology of nanocomposites based on SR/EPDM blends compatibilized by maleic anhydride, Polymer 113 (2017) 156-166.
[17] M. Narasimhan, M. Chandrasekaran, S. Govindasamy, A. Aravamudhan, Heterogeneous nanocatalysts for sustainable biodiesel production: A review, Journal of Environmental Chemical Engineering 9(1) (2021) 104876.
[18] M. Shokouhimehr, Magnetically separable and sustainable nanostructured catalysts for heterogeneous reduction of nitroaromatics, Catalysts 5(2) (2015) 534-560.
[19] Tripathi, S., Boggs, W. Role of Nanocatalysts in Synthesis of Carbon Nanofiber. In Carbon Nanofibers: Fundamentals and Applications; Elsevier: Amsterdam, Netherlands, 2021; pp. 49–70.
[20] R. Naveenkumar, G. Baskar, Process optimization, green chemistry balance and technoeconomic analysis of biodiesel production from castor oil using heterogeneous nanocatalyst, Bioresource Technology 320(Part A) (2021) 124347.
[21] S.B. Singh, P.K. Tandon, Catalysis: a brief review on nano-catalyst, Journal of Energy and Chemical Engineering 2(3) (2014) 106-115.
[22] S. Kazemifard, H. Nayebzadeh, N. Saghatoleslami, E. Safakish, Application of magnetic alumina-ferric oxide nanocatalyst supported by KOH for in-situ transesterification of microalgae cultivated in wastewater medium, Biomass and Bioenergy 129 (2019) 105338.
[23] A. Marjani, M.H. Zare, M.H. Sadeghi, S. Shirazian, M. Ghadiri, Synthesis of alginate-coated magnetic nanocatalyst containing high-performance integrated enzyme for phenol removal, Journal of Environmental Chemical Engineering 9(1) (2021) 104884.
[24] F. Sadegh, N. Politakos, E.G. de San Román, O. Sanz, I. Perez-Miqueo, S.E. Moya, R. Tomovska, A green synthesis of nanocatalysts based on reduced graphene oxide/magnetic nanoparticles for the degradation of Acid Red 1, Royal Society of Chemistry Advances 10(64) (2020) 38805-38817.
[25] A.S. Ethiraj, P. Uttam, K. Varunkumar, K.F. Chong, G.A. Ali, Photocatalytic performance of a novel semiconductor nanocatalyst: Copper doped nickel oxide for phenol degradation, Materials Chemistry and Physics 242(0) (2020) 122520.
[26] A.S. Ethiraj, P. Uttam, V. K, K.F. Chong, G.A.M. Ali, Photocatalytic performance of a novel semiconductor nanocatalyst: Copper doped nickel oxide for phenol degradation, Materials Chemistry and Physics 242 (2020) 122520.
[27] T. Jayabalan, S. Naina Mohamed, M. Matheswaran, T. Radhakrishnan, A. Pugazhendhi, A. Alagarsamy, Enhanced biohydrogen production from sugar industry effluent using nickel oxide and cobalt oxide as cathode nanocatalysts in microbial electrolysis cell, International Journal of Energy Research 45(12) (2020) 17431-17439.
[28] A.S. Adekunle, J.A. Oyekunle, L.M. Durosinmi, O.S. Oluwafemi, D.S. Olayanju, A.S. Akinola, O.R. Obisesan, O.F. Akinyele, T.A. Ajayeoba, Potential of cobalt and cobalt oxide nanoparticles as nanocatalyst towards dyes degradation in wastewater, Nano-Structures & Nano-Objects 21 (2020) 100405.
[29] C.-O.O. Maureen, O.J. Nnaemeka, A.N. Basil, O.E. Emeka, Photocatalytic degradation of a basic dye using zinc oxide nanocatalyst, International Letters of Chemistry, Physics and Astronomy 81 (2019) 18-26.
[30] L. Pandian, R. Rajasekaran, P. Govindan, Synergistic effect of ozone on cadmium doped zinc oxide nanocatalyst for the degradation of textile dyeing wastewater, Materials Research Express 6(8) (2019) 085513.
[31] Q. Sun, X. Fu, R. Si, C.H. Wang, N. Yan, Mesoporous silica-encaged ultrafine bimetallic nanocatalysts for CO_2 hydrogenation to formates, ChemCatChem 11(20) (2019) 5093-5097.
[32] P.C.L. Muraro, S.R. Mortari, B.S. Vizzotto, G. Chuy, C. Dos Santos, L.F.W. Brum, W.L. da Silva, Iron oxide nanocatalyst with titanium and silver nanoparticles: Synthesis, characterization and photocatalytic activity on the degradation of Rhodamine B dye, Scientific reports 10(1) (2020) 1-9.
[33] Z. Cheng, X. Chu, J. Yin, B. Dai, W. Zhao, Y. Jiang, J. Xu, H. Zhong, P. Zhao, L. Zhang, Formation of composite fuels by coating aluminum powder with a cobalt nanocatalyst: Enhanced heat release and catalytic performance, Chemical Engineering Journal 385 (2020) 123859.
[34] G. Jaiswal, V.G. Landge, D. Jagadeesan, E. Balaraman, Iron-based nanocatalyst for the acceptorless dehydrogenation reactions, Nature communications 8(1) (2017) 1-13.
[35] K. Zhang, J.H. Cha, S.Y. Jeon, K.O. Kirlikovali, M. Ostadhassan, V. Rasouli, O.K. Farha, H.W. Jang, R.S. Varma, M. Shokouhimehr, Pd modified prussian blue frameworks: Multiple electron transfer pathways for improving catalytic activity toward hydrogenation of nitroaromatics, Molecular Catalysis 492(0) (2020) 110967.
[36] H. Suo, L. Xu, Y. Xue, X. Qiu, H. Huang, Y. Hu, Ionic liquids-modified cellulose coated magnetic nanoparticles for enzyme immobilization: improvement of catalytic performance, Carbohydrate polymers 234(0) (2020) 115914.
[37] K. Yan, C. Jarvis, T. Lafleur, Y. Qiao, X. Xie, Novel synthesis of Pd nanoparticles for hydrogenation of biomass-derived platform chemicals showing enhanced catalytic performance, RSC advances 3(48) (2013) 25865-25871.
[38] K. Yan, T. Lafleur, G. Wu, J. Liao, C. Ceng, X. Xie, Highly selective production of value-added γ-valerolactone from biomass-derived levulinic acid using the robust Pd nanoparticles, Applied Catalysis A: General 468(0) (2013) 52-58.
[39] M. Shokouhimehr, K. Hong, T.H. Lee, C.W. Moon, S.P. Hong, K. Zhang, J.M. Suh, K.S. Choi, R.S. Varma, H.W. Jang, Magnetically retrievable nanocomposite adorned with Pd nanocatalysts: efficient reduction of nitroaromatics in aqueous media, Green Chemistry 20(16) (2018) 3809-3817.
[40] S. Luo, Z. Zeng, G. Zeng, Z. Liu, R. Xiao, M. Chen, L. Tang, W. Tang, C. Lai, M. Cheng, Metal organic frameworks as robust host of palladium nanoparticles in heterogeneous catalysis: Synthesis, application, and prospect, ACS applied materials & interfaces 11(36) (2019) 32579-32598.
[41] M.J. Ndolomingo, N. Bingwa, R. Meijboom, Review of supported metal nanoparticles: synthesis methodologies, advantages and application as catalysts, Journal of Materials Science 55(15) (2020) 6195-6241.
[42] K. Yan, T. Lafleur, C. Jarvis, G. Wu, Clean and selective production of γ-valerolactone from biomass-derived levulinic acid catalyzed by recyclable Pd

nanoparticle catalyst, Journal of cleaner production 72(0) (2014) 230-232.
[43] B.R. Cuenya, Synthesis and catalytic properties of metal nanoparticles: Size, shape, support, composition, and oxidation state effects, Thin Solid Films 518(12) (2010) 3127-3150.
[44] M.B. Gawande, A.K. Rathi, P.S. Branco, I.D. Nogueira, A. Velhinho, J.J. Shrikhande, U.U. Indulkar, R.V. Jayaram, C.A.A. Ghumman, N. Bundaleski, Regio-and Chemoselective Reduction of Nitroarenes and Carbonyl Compounds over Recyclable Magnetic Ferrite-Nickel Nanoparticles (Fe_3O_4/Ni) by Using Glycerol as a Hydrogen Source, Chemistry–A European Journal 18(40) (2012) 12628-12632.
[45] M.B. Gawande, A. Rathi, I.D. Nogueira, C. Ghumman, N. Bundaleski, O. Teodoro, P.S. Branco, A Recyclable ferrite–Co magnetic nanocatalyst for the oxidation of alcohols to carbonyl compounds, ChemPlusChem 77(10) (2012) 865-871.
[46] F. Sharifianjazi, M. Moradi, N. Parvin, A. Nemati, A.J. Rad, N. Sheysi, A. Abouchenari, A. Mohammadi, S. Karbasi, Z. Ahmadi, Magnetic $CoFe_2O_4$ nanoparticles doped with metal ions: a review, Ceramics International 46(11 Part B) (2020) 18391-18412.
[47] J. Feng, L. Su, Y. Ma, C. Ren, Q. Guo, X. Chen, $CuFe_2O_4$ magnetic nanoparticles: A simple and efficient catalyst for the reduction of nitrophenol, Chemical engineering journal 221(0) (2013) 16-24.
[48] Y. Li, J. Shen, Y. Hu, S. Qiu, G. Min, Z. Song, Z. Sun, C. Li, General flame approach to chainlike MFe_2O_4 spinel (M= Cu, Ni, Co, Zn) nanoaggregates for reduction of nitroaromatic compounds, Industrial & Engineering Chemistry Research 54(40) (2015) 9750-9757.
[49] A. Goyal, S. Bansal, S. Singhal, Facile reduction of nitrophenols: Comparative catalytic efficiency of MFe_2O_4 (M= Ni, Cu, Zn) nano ferrites, International journal of hydrogen energy 39(10) (2014) 4895-4908.
[50] A. Goyal, S. Bansal, V. Kumar, J. Singh, S. Singhal, Mn substituted cobalt ferrites ($CoMnxFe_{2-x}O_4$ (x= 0.0, 0.2, 0.4, 0.6, 0.8, 1.0)): As magnetically separable heterogeneous nanocatalyst for the reduction of nitrophenols, Applied Surface Science 324(0) (2015) 877-889.
[51] V.S. Kiran, S. Sumathi, Comparison of catalytic activity of bismuth substituted cobalt ferrite nanoparticles synthesized by combustion and co-precipitation method, Journal of Magnetism and Magnetic Materials 421(0) (2017) 113-119.
[52] C. Singh, A. Goyal, S. Singhal, Nickel-doped cobalt ferrite nanoparticles: efficient catalysts for the reduction of nitroaromatic compounds and photo-oxidative degradation of toxic dyes, Nanoscale 6(14) (2014) 7959-7970.
[53] C. Dey, A. Chaudhuri, A. Ghosh, M. Mandal Goswami, Magnetic cube-shaped $NiFe_2O_4$ nanoparticles: an effective model catalyst for nitro compound reduction, ChemCatChem 9(11) (2017) 1953-1959.
[54] M. Dhiman, A. Goyal, V. Kumar, S. Singhal, Designing different morphologies of $NiFe_2O_4$ for tuning of structural, optical and magnetic properties for catalytic advancements, New Journal of Chemistry 40(12) (2016) 10418-10431.
[55] I. Papadas, K. Subrahmanyam, M.G. Kanatzidis, G. Armatas, Templated assembly of $BiFeO_3$ nanocrystals into 3D mesoporous networks for catalytic applications, Nanoscale 7(13) (2015) 5737-5743.
[56] M. Amir, U. Kurtan, A. Baykal, Rapid color degradation of organic dyes by Fe_3O_4@His@Ag recyclable magnetic nanocatalyst, Journal of Industrial and Engineering Chemistry 27(0) (2015) 347-353.
[57] U. Kurtan, M. Amir, A. Yıldız, A. Baykal, Synthesis of magnetically recyclable $MnFe_2O_4$@SiO_2@Ag nanocatalyst: Its high catalytic performances for azo dyes and nitro compounds reduction, Applied Surface Science 376(0) (2016) 16-25.
[58] P. Mohammadi, H. Sheibani, Green synthesis of Fe_3O_4@SiO_2-Ag magnetic nanocatalyst using safflower extract and its application as recoverable catalyst for reduction of dye pollutants in water, Applied Organometallic Chemistry 32(4) (2018) e4249.
[59] H. Veisi, S. Razeghi, P. Mohammadi, S. Hemmati, Silver nanoparticles decorated on thiol-modified magnetite nanoparticles (Fe_3O_4/SiO_2-Pr-S-Ag) as a recyclable nanocatalyst for degradation of organic dyes, Materials Science and Engineering: C 97 (2019) 624-631.
[60] B.K. Ghosh, D. Moitra, M. Chandel, H. Lulla, N.N. Ghosh, Ag nanoparticle immobilized mesoporous TiO_2-cobalt ferrite nanocatalyst: A highly active, versatile, magnetically separable and reusable catalyst, Materials Research Bulletin 94 (2017) 361-370.
[61] M.S. Najafinejad, P. Mohammadi, M. Mehdi Afsahi, H. Sheibani, Biosynthesis of Au nanoparticles supported on Fe_3O_4@polyaniline as a heterogeneous and reusable magnetic nanocatalyst for reduction of the azo dyes at ambient temperature, Materials Science and Engineering: C 98 (2019) 19-29.
[62] P.L.d. Oliveira, N.S. Lima, A.C.F.d.M. Costa, E.B. Cavalcanti, L.d.S. Conrado, Obtaining TiO_2:$CoFe_2O_4$ nanocatalyst by Pechini method for diuron degradation and mineralization, Ceramics International 46(7) (2020) 9421-9435.
[63] H.H. Mohamed, N.A. Alomair, S. Akhtar, T.E. Youssef, Eco-friendly synthesized α-Fe_2O_3/TiO_2 heterojunction with enhanced visible light photocatalytic activity, Journal of Photochemistry and Photobiology A: Chemistry 382 (2019) 111951.
[64] R. Ranjith, V. Renganathan, S.-M. Chen, N.S. Selvan, P.S. Rajam, Green synthesis of reduced graphene oxide supported TiO_2/Co_3O_4 nanocomposite for photocatalytic degradation of methylene blue and crystal violet, Ceramics International 45(10) (2019) 12926-12933.
[65] V. Vetere, A.B. Merlo, M.L. Casella, Chemoselective hydrogenation of aromatic ketones with Pt-based heterogeneous catalysts. Substituent effects, Applied Catalysis A: General 491 (2015) 70-77.
[66] W. Jin, L. Pastor-Pérez, J.J. Villora-Pico, M.M. Pastor-Blas, A. Sepúlveda-Escribano, S. Gu, N.D. Charisiou, K. Papageridis, M.A. Goula, T.R. Reina, Catalytic conversion of palm oil to bio-hydrogenated diesel over novel N-doped activated carbon supported Pt nanoparticles, Energies 13(1) (2020) 132.
[67] H.M.A. Sharif, A. Mahmood, H.Y. Cheng, R. Djellabi, J. Ali, W.L. Jiang, S.S. Wang, M.R. Haider, N. Mahmood, A.J. Wang, Fe_3O_4 nanoparticles coated with EDTA and Ag nanoparticles for the catalytic reduction of organic dyes from wastewater, ACS Applied Nano Materials 2(8) (2019) 5310-5319.
[68] G.P. Sahoo, D.K. Bhui, D. Das, A. Misra, Synthesis of anisotropic gold nanoparticles and their catalytic activities of breaking azo bond in sudan-1, Journal of Molecular Liquids 198 (2014) 215-222.
[69] Z.H. Xie, H.Y. Zhou, C.S. He, Z.C. Pan, G. Yao, B. Lai, Synthesis, application and catalytic performance of layered double hydroxide based catalysts in advanced oxidation processes for wastewater decontamination: A review, Chemical Engineering Journal 414(0) (2021) 128713.
[70] X.Y. Zhang, W.L. Yu, J. Zhao, B. Dong, C.G. Liu, Y.M. Chai, Recent development on self-supported transition metal-based catalysts for water electrolysis at large current density, Applied Materialstoday 22 (2021) 100913.
[71] M.S. Holden, K.E. Nick, M. Hall, J.R. Milligan, Q. Chen, C.C. Perry, Synthesis and catalytic activity of pluronic stabilized silver–gold bimetallic nanoparticles, RSC advances 4(94) (2014) 52279-52288.
[72] S.G. Babu, M. Gopiraman, D. Deng, K. Wei, R. Karvembu, I.S. Kim, Robust Au–Ag/graphene bimetallic nanocatalyst for multifunctional activity with high synergism, Chemical Engineering Journal 300 (2016) 146-159.
[73] N.V. Long, M. Ohtaki, T.D. Hien, J. Randy, M. Nogami, A comparative study of Pt and Pt–Pd core–shell nanocatalysts, Electrochimica Acta 56(25) (2011) 9133-9143.
[74] Z. Bo, X. Guo, X. Wei, H. Yang, J. Yan, K. Cen, Density functional theory calculations of NO_2 and H_2S adsorption on the group 10 transition metal (Ni, Pd and Pt) decorated graphene, Physica E: Low-dimensional Systems and Nanostructures 109 (2019) 156-163.
[75] K. Patel, S. Kapoor, D.P. Dave, T. Mukherjee, Synthesis of Pt, Pd, Pt/Ag and Pd/Ag nanoparticles by microwave-polyol method, Journal of Chemical Sciences 117(4) (2005) 311-316.
[76] B.H. Susanto, J.R.V. Siallagan, Analysis of NiMoP/γ-Al_2O_3 Catalyst Preparation with Impregnation and Microwave Polyol Methods for Bio-Jet Production, Materials Science Forum 1000 (2020) 257-264
[77] H. Gu, Y. Yang, J. Tian, G. Shi, Photochemical synthesis of noble metal (Ag, Pd, Au, Pt) on graphene/ZnO multihybrid nanoarchitectures as electrocatalysis for H2O2 reduction, ACS applied materials & interfaces 5(14) (2013) 6762-6768.
[78] T. Iqbal, S. Tufail, S. Ghazal, Synthesis of silver, chromium, manganese, tin and iron nano particles by different techniques, International Journal of Nanoscience and Nanotechnology 13(1) (2017) 19-52.
[79] M.A. Salem, E.A. Bakr, H.G. El-Attar, Pt@ Ag and Pd@ Ag core/shell nanoparticles for catalytic degradation of Congo red in aqueous solution, Spectrochimica Acta Part A: Molecular and Biomolecular Spectroscopy 188 (2018) 155-163.
[80] M. Moradi, M. Haghighi, S. Allahyari, Precipitation dispersion of Ag–ZnO nanocatalyst over functionalized multiwall carbon nanotube used in degradation of Acid Orange from wastewater, Process Safety and Environmental Protection 107 (2017) 414-427.
[81] C. Duan, C. Liu, X. Meng, W. Lu, Y. Ni, Fabrication of carboxymethylated cellulose fibers supporting Ag NPs@MOF-199s nanocatalysts for catalytic reduction of 4-nitrophenol, Applied Organometallic Chemistry 33(5) (2019) e4865.
[82] K. Iqbal, A. Iqbal, A.M. Kirillov, B. Wang, W. Liu, Y. Tang, A new Ce-doped MgAl-LDH@ Au nanocatalyst for highly efficient reductive degradation of organic contaminants, Journal of Materials Chemistry A 5(14) (2017) 6716-6724.
[83] A. Sahoo, S.K. Tripathy, N. Dehury, S. Patra, A porous trimetallic Au@ Pd@ Ru nanoparticle system: synthesis, characterisation and efficient dye degradation and removal, Journal of Materials Chemistry A 3(38) (2015) 19376-19383.
[84] M. Nasrollahzadeh, T. Baran, N.Y. Baran, M. Sajjadi, M.R. Tahsili, M. Shokouhimehr, Pd nanocatalyst stabilized on amine-modified zeolite: Antibacterial and

catalytic activities for environmental pollution remediation in aqueous medium, Separation and Purification Technology 239 (2020) 116542.
[85] Q. Yan, X.Y. Wang, J.J. Feng, L.P. Mei, A.J. Wang, Simple fabrication of bimetallic platinum-rhodium alloyed nanomultipods: A highly effective and recyclable catalyst for reduction of 4-nitrophenol and rhodamine B, Journal of Colloid and Interface Science 582(Part B) (2021) 701-710.
[86] V. Katoch, N. Sharma, M. Sharma, M. Baghoria, J.J. Panda, M. Singh, B. Prakash, Microflow synthesis and enhanced photocatalytic dye degradation performance of antibacterial Bi_2O_3 nanoparticles, Environmental Science and Pollution Research 28(15) (2021) 1-11.
[87] Y. Dang, Y. Cheng, Y. Zhou, Y. Huang, K. Wang, Nano-PAA-CuCl2 Composite as Fenton-like Reusable Catalyst to Enhanced Degrade Organic Pollutant MB/MO, Catalysts 11(1) (2021) 10.
[88] A. ur Rehman, M. Aadil, S. Zulfiqar, P.O. Agboola, I. Shakir, M.F. Aly Aboud, S. Haider, M.F. Warsi, Fabrication of binary metal doped CuO nanocatalyst and their application for the industrial effluents treatment, Ceramics International 47(5) (2021) 5929-5937.
[89] S. Dehghan, M. Tahergorabi, S. Norzaee, E. Boorboor Azimi, M. Hasham Firooz, Y. Dadban Shahamat, Preparation and photocatalytic performance of reduced graphene oxide/ ZnO nanocatalyst for degradation of metalaxyl from aqueous solution: effect of operational parameters, mineralisation and toxicity bioassay, International Journal of Environmental Analytical Chemistry 102(18) (2022) 7112-7134.
[90] M. Dorosti, M. Baghdadi, S. Nasimi, A continuous electroreduction cell composed of palladium nanocatalyst immobilized on discarded cigarette filters as an active bed for Cr(VI) removal from groundwater, Journal of Environmental Management 264 (2020) 110409.
[91] S.G. Shelar, V.K. Mahajan, S.P. Patil, G.H. Sonawane, Effect of doping parameters on photocatalytic degradation of methylene blue using Ag doped ZnO nanocatalyst, SN Applied Sciences 2(5) (2020) 820.
[92] M. Ikram, M.I. Khan, A. Raza, M. Imran, A. Ul-Hamid, S. Ali, Outstanding performance of silver-decorated MoS_2 nanopetals used as nanocatalyst for synthetic dye degradation, Physica E: Low-dimensional Systems and Nanostructures 124 (2020) 114246.
[93] M. Nasrollahzadeh, R. Akbari, Z. Issaabadi, S.M. Sajadi, Biosynthesis and characterization of Ag/MgO nanocomposite and its catalytic performance in the rapid treatment of environmental contaminants, Ceramics International 46(2) (2020) 2093-2101.
[94] M. Khoshnamvand, C. Huo, J. Liu, Silver nanoparticles synthesized using Allium ampeloprasum L. leaf extract: Characterization and performance in catalytic reduction of 4-nitrophenol and antioxidant activity, Journal of Molecular Structure 1175 (2019) 90-96.
[95] B. Kumar, K.S. Vizuete, V. Sharma, A. Debut, L. Cumbal, Ecofriendly synthesis of monodispersed silver nanoparticles using Andean Mortiño berry as reductant and its photocatalytic activity, Vacuum 160 (2019) 272-278.
[96] V. Garole, B. Choudhary, S. Tetgure, D. Garole, A. Borse, Palladium nanocatalyst: green synthesis, characterization, and catalytic application, International Journal of Environmental Science and Technology 16(12) (2019) 7885-7892.
[97] M. Hashemi Salehi, M. Yousefi, M. Hekmati, E. Balali, Application of palladium nanoparticle-decorated Artemisia abrotanum extract-modified graphene oxide for highly active catalytic reduction of methylene blue, methyl orange and rhodamine B, Applied Organometallic Chemistry 33(10) (2019) e5123.
[98] Z.U.H. Khan, H.M. Sadiq, N.S. Shah, A.U. Khan, N. Muhammad, S.U. Hassan, K. Tahir, F.U. Khan, M. Imran, N. Ahmad, Greener synthesis of zinc oxide nanoparticles using Trianthema portulacastrum extract and evaluation of its photocatalytic and biological applications, Journal of Photochemistry and Photobiology B: Biology 192 (2019) 147-157.
[99] M. Ganesh, S.G. Lee, J. Jayaprakash, M. Mohankumar, H.T. Jang, Hydnocarpus alpina Wt extract mediated green synthesis of ZnO nanoparticle and screening of its anti-microbial, free radical scavenging, and photocatalytic activity, Biocatalysis and agricultural biotechnology 19 (2019) 101129.
[100] A.R. Prasad, J. Garvasis, S.K. Oruvil, A. Joseph, Bio-inspired green synthesis of zinc oxide nanoparticles using Abelmoschus esculentus mucilage and selective degradation of cationic dye pollutants, Journal of Physics and Chemistry of Solids 127 (2019) 265-274.
[101] K. Rajendaran, R. Muthuramalingam, S. Ayyadurai, Green synthesis of Ag-Mo/CuO nanoparticles using Azadirachta indica leaf extracts to study its solar photocatalytic and antimicrobial activities, Materials Science in Semiconductor Processing 91 (2019) 230-238.
[102] P. Mohammadi, H. Daneshafruz, H. Sheibani, Gold nanoparticles on cyanuric citric acid functionalized magnetic SBA-16 as an effective catalyst for dye reduction, Physica E: Low-dimensional Systems and Nanostructures 126 (2021) 114392.
[103] M. Memar, A.R. Rezvani, S. Saheli, Synthesis, characterization, and application of CuO nanoparticle 2D doped with Zn^{2+} against photodegradation of organic dyes (MB & MO) under sunlight, Journal of Materials Science: Materials in Electronics (2021) 1-19.
[104] A. Nouri, B. Faraji Dizaji, N. Kianinejad, A. Jafari Rad, S. Rahimi, M. Irani, F. Sharifian Jazi, Simultaneous linear release of folic acid and doxorubicin from ethyl cellulose/chitosan/g-C_3N_4/MoS_2 core-shell nanofibers and its anticancer properties, Journal of Biomedical Materials Research Part A 109(6) (2021) 903-914.
[105] S. Yuan, G. Zhang, J. Zhu, N. Mamrol, S. Liu, Z. Mai, P. Van Puyvelde, B. Van der Bruggen, Hydrogel assisted interfacial polymerization for advanced nanofiltration membranes, Journal of Materials Chemistry A 8(6) (2020) 3238-3245.
[106] X. Li, S. Ye, Y.C. Zhang, H.P. Zhao, Y. Huang, B. Zhang, T. Cai, Magnetic Janus nanocomposites with iridium (III) complexes for heterogeneous catalysis of logic controlled RAFT polymerization using multiplexed external switching, Nanoscale 12(14) (2020) 7595-7603.
[107] H. Hu, J.H. Xin, H. Hu, PAM/graphene/Ag ternary hydrogel: synthesis, characterization and catalytic application, Journal of Materials Chemistry A 2(29) (2014) 11319-11333.
[108] F. Gorginpour, H. Zali-Boeini, H.A. Rudbari, A quinoxaline-based porous organic polymer containing copper nanoparticles CuNPs@ Q-POP as a robust nanocatalyst toward C–N coupling reaction, RSC Advances 11(6) (2021) 3655-3665.
[109] L. Ai, J. Jiang, Catalytic reduction of 4-nitrophenol by silver nanoparticles stabilized on environmentally benign macroscopic biopolymer hydrogel, Bioresource technology 132 (2013) 374-377.
[110] M. Norouzi, D. Elhamifar, Ionic liquid-modified magnetic mesoporous silica supported tungstate: A powerful and magnetically recoverable nanocatalyst, Composites Part B: Engineering 176 (2019) 107308.
[111] Y. Mei, Y. Lu, F. Polzer, M. Ballauff, M. Drechsler, Catalytic activity of palladium nanoparticles encapsulated in spherical polyelectrolyte brushes and core–shell microgels, Chemistry of Materials 19(5) (2007) 1062-1069.
[112] M.I. Din, R. Khalid, Z. Hussain, T. Hussain, A. Mujahid, J. Najeeb, F. Izhar, Nanocatalytic assemblies for catalytic reduction of nitrophenols: a critical review, Critical reviews in analytical chemistry 50(4) (2020) 322-338.
[113] M. J. Thiele, M.D. Davari, M. Konig, I. Hofmann, N.O. Junker, T. Mirzaei Garakani, L. Vojcic, J.r. Fitter, U. Schwaneberg, Enzyme–polyelectrolyte complexes boost the catalytic performance of enzymes, ACS catalysis 8(11) (2018) 10876-10887.
[114] C. Nagahama, A. Zinchenko, Small DNA additives to polyelectrolyte multilayers promote formation of ultrafine gold nanoparticles with enhanced catalytic activity, Colloid and Polymer Science 297(3) (2019) 363-369.
[115] M. Ajmal, M. Siddiq, H. Al-Lohedan, N. Sahiner, Highly versatile p (MAc)–M (M: Cu, Co, Ni) microgel composite catalyst for individual and simultaneous catalytic reduction of nitro compounds and dyes, RSC Advances 4(103) (2014) 59562-59570.
[116] N. Sahiner, S. Yildiz, H. Al-Lohedan, The resourcefulness of p (4-VP) cryogels as template for in situ nanoparticle preparation of various metals and their use in H_2 production, nitro compound reduction and dye degradation, Applied Catalysis B: Environmental 166-167 (2015) 145-154.
[117] R.K. Narayanan, S.J. Devaki, T.P. Rao, Robust fibrillar nanocatalysts based on silver nanoparticle-entrapped polymeric hydrogels, Applied Catalysis A: General 483 (2014) 31-40.
[118] S. Saha, A. Pal, S. Kundu, S. Basu, T. Pal, Photochemical green synthesis of calcium-alginate-stabilized Ag and Au nanoparticles and their catalytic application to 4-nitrophenol reduction, Langmuir 26(4) (2010) 2885-2893.
[119] D. Hu, Y. Huang, H. Liu, H. Wang, S. Wang, M. Shen, M. Zhu, X. Shi, The assembly of dendrimer-stabilized gold nanoparticles onto electrospun polymer nanofibers for catalytic applications, Journal of Materials Chemistry A 2(7) (2014) 2323-2332.
[120] S. Gatard, L. Salmon, C. Deraedt, J. Ruiz, D. Astruc, S. Bouquillon, Gold Nanoparticles Stabilized by Glycodendrimers: Synthesis and Application to the Catalytic Reduction of 4-Nitrophenol, European Journal of Inorganic Chemistry 2014(16) (2014) 2671-2677.
[121] K. Kuroda, T. Ishida, M. Haruta, Reduction of 4-nitrophenol to 4-aminophenol over Au nanoparticles deposited on PMMA, Journal of Molecular Catalysis A: Chemical 298(1-2) (2009) 7-11.
[122] P. Kannan, F.A. Rahim, X. Teng, R. Chen, H. Sun, L. Huang, D.-H. Kim, Enhanced emission of NaYF4: Yb, Er/Tm nanoparticles by selective growth of Au and Ag nanoshells, RSC advances 3(21) (2013) 7718-7721.
[123] C. Zhang, Q. Yang, N. Zhan, L. Sun, H. Wang, Y. Song, Y. Li, Silver nanopar-

ticles grown on the surface of PAN nanofiber: Preparation, characterization and catalytic performance, Colloids and Surfaces A: Physicochemical and Engineering Aspects 362(1-3) (2010) 58-64.
[124] S. Harish, J. Mathiyarasu, K. Phani, V. Yegnaraman, Synthesis of conducting polymer supported Pd nanoparticles in aqueous medium and catalytic activity towards 4-nitrophenol reduction, Catalysis letters 128(1) (2009) 197-202.
[125] T. Yao, T. Cui, H. Wang, L. Xu, F. Cui, J. Wu, A simple way to prepare Au@ polypyrrole/Fe_3O_4 hollow capsules with high stability and their application in catalytic reduction of methylene blue dye, Nanoscale 6(13) (2014) 7666-7674.
[126] K.Ö. Hamaloğlu, E. Sağ, Ç. Kip, E. Şenlik, B.S. Kaya, A. Tuncel, Magnetic-porous microspheres with synergistic catalytic activity of small-sized gold nanoparticles and titania matrix, Frontiers of Chemical Science and Engineering 13(3) (2019) 574-585.
[127] S. Panigrahi, S. Basu, S. Praharaj, S. Pande, S. Jana, A. Pal, S.K. Ghosh, T. Pal, Synthesis and size-selective catalysis by supported gold nanoparticles: study on heterogeneous and homogeneous catalytic process, The Journal of Physical Chemistry C 111(12) (2007) 4596-4605.
[128] I.U.H. Bhat, M.N.K. Anwar, J.N. Appaturi, Polymer based palladium nanocatalyst for the degradation of nitrate and Congo Red, Journal of Polymers and the Environment 27(7) (2019) 1475-1487.
[129] B. Samai, S.C. Bhattacharya, Conducting polymer supported cerium oxide nanoparticle: Enhanced photocatalytic activity for waste water treatment, Materials Chemistry and Physics 220 (2018) 171-181.
[130] L. Kaliraj, J.C. Ahn, E.J. Rupa, S. Abid, J. Lu, D.C. Yang, Synthesis of panos extract mediated ZnO nano-flowers as photocatalyst for industrial dye degradation by UV illumination, Journal of Photochemistry and Photobiology B: Biology 199 (2019) 111588.
[131] M. Nasrollahzadeh, B. Jaleh, T. Baran, R.S. Varma, Efficient degradation of environmental contaminants using Pd-RGO nanocomposite as a retrievable catalyst, Clean Technologies and Environmental Policy 22(2) (2020) 325-335.
[132] X. Peng, X. Bai, Z. Cui, X. Liu, Green synthesis of Pd truncated octahedrons using of firmiana simplex leaf extract and their catalytic study for electro-oxidation of methanol and reduction of p-nitrophenol, Applied Organometallic Chemistry 33(8) (2019) e5045.
[133] S. Bao, H. Liu, Y. Liu, W. Yang, Y. Wang, Y. Yu, Y. Sun, K. Li, Amino-functionalized graphene oxide-supported networked Pd–Ag nanowires as highly efficient catalyst for reducing Cr(VI) in industrial effluent by formic acid, Chemosphere 257 (2020) 127245.
[134] M.N. Chong, B. Jin, C.W. Chow, C. Saint, Recent developments in photocatalytic water treatment technology: a review, Water research 44(10) (2010) 2997-3027.
[135] A. Jaafara, A. Driouichb, Z. Lakbaibib, H.B. El Ayouchiac, K. Azzaouid, A. Boussaouda, S. Jodehe, Central composite design for the optimization of Basic Red V degradation in aqueous solution using Fenton reaction, Desalination and Water Treatment 158 (2019) 364-371.
[136] A. Jaafar, H.B. El Ayouchia, Z. Lakbaibi, A. Boussaoud, S. Jodeh, K. Azzaoui, M. Tabyaoui, Degradation of Pollutant Dye in Aqueous Solution using Fenton Reaction: A DFT Study, G P Globalize Research Journal of Chemistry 3(1) (2019) 53-61.
[137] H. Eskandarloo, A. Kierulf, A. Abbaspourrad, Nano-and micromotors for cleaning polluted waters: focused review on pollutant removal mechanisms, Nanoscale 9(37) (2017) 13850-13863.
[138] K. Shivaji, E.S. Monica, A. Devadoss, D.D. Kirubakaran, C.R. Dhas, S.M. Jain, S. Pitchaimuthu, Synthesizing Green Photocatalyst Using Plant Leaf Extract for Water Pollutant Treatment, in: M. Naushad, S. Rajendran, E. Lichtfouse (Eds.), Green Photocatalysts, Springer International Publishing, Cham, 2020, pp. 25-46.
[139] A.A. Yaqoob, T. Parveen, K. Umar, M.N. Mohamad Ibrahim, Role of nanomaterials in the treatment of wastewater: A review, Water 12(2) (2020) 495.
[140] A. Moghanian, F. Sharifianjazi, P. Abachi, E. Sadeghi, H. Jafarikhorami, A. Sedghi, Production and properties of Cu/TiO_2 nano-composites, Journal of Alloys and Compounds 698 (2017) 518-524.
[141] S. Kabra, S. Gharde, P. Gore, S. Jain, V.H. Khire, B. Kandasubramanian, Recent trends in nanothermites: Fabrication, characteristics and applications, Nano Express 1(3) (2020) 032001.
[142] T. Toyao, M. Saito, Y. Horiuchi, K. Mochizuki, M. Iwata, H. Higashimura, M. Matsuoka, Efficient hydrogen production and photocatalytic reduction of nitrobenzene over a visible-light-responsive metal–organic framework photocatalyst, Catalysis Science & Technology 3(8) (2013) 2092-2097.
[143] Y. Pi, X. Li, Q. Xia, J. Wu, Y. Li, J. Xiao, Z. Li, Adsorptive and photocatalytic removal of Persistent Organic Pollutants (POPs) in water by metal-organic frameworks (MOFs), Chemical Engineering Journal 337 (2018) 351-371.
[144] T. Saeed, A. Naeem, I.U. Din, M.A. Alotaibi, A.I. Alharthi, I.W. Khan, N.H. Khan, T. Malik, Structure, nomenclature and viable synthesis of micro/nanoscale metal organic frameworks and their remarkable applications in adsorption of organic pollutants, Microchemical Journal 159 (2020) 105579.
[145] M. Nasrollahzadeh, M. Sajjadi, S. Iravani, R.S. Varma, Green-synthesized nanocatalysts and nanomaterials for water treatment: Current challenges and future perspectives, Journal of Hazardous Materials 401 (2021) 123401.
[146] A. Mukhtar, S. Ullah, A.G. Al-Sehemi, M.A. Assiri, S. Saqib, R. Amen, M. Babar, M.A. Bustam, T. Ahmad, Synthesis and Stability of Metal-organic Frameworks (MOFs) Photocatalysts for the Removal of Persistent Organic Pollutants (POPs) from Wastewater, Current Analytical Chemistry 17(1) (2021) 61-81.
[147] F.S. Jazi, N. Parvin, M. Rabiei, M. Tahriri, Z.M. Shabestari, A.R. Azadmehr, Effect of the synthesis route on the grain size and morphology of ZnO/Ag nanocomposite, Journal of Ceramic Processing Research 13(5) (2012) 523-526.
[148] Y. Zhang, J. Zhou, X. Chen, Q. Feng, W. Cai, MOF-derived C-doped ZnO composites for enhanced photocatalytic performance under visible light, Journal of Alloys and Compounds 777 (2019) 109-118.
[149] M.C. Das, H. Xu, Z. Wang, G. Srinivas, W. Zhou, Y.-F. Yue, V.N. Nesterov, G. Qian, B. Chen, A Zn_4O-containing doubly interpenetrated porous metal–organic framework for photocatalytic decomposition of methyl orange, Chemical Communications 47(42) (2011) 11715-11717.
[150] T. Parandhaman, N. Pentela, B. Ramalingam, D. Samanta, S.K. Das, Metal nanoparticle loaded magnetic-chitosan microsphere: water dispersible and easily separable hybrid metal nano-biomaterial for catalytic applications, ACS Sustainable Chemistry & Engineering 5(1) (2017) 489-501.
[151] M. Abdeen, S. Sabry, H. Ghozlan, A.A. El-Gendy, E.E. Carpenter, Microbial-physical synthesis of Fe and Fe_3O_4 magnetic nanoparticles using Aspergillus niger YESM1 and supercritical condition of ethanol, Journal of Nanomaterials 2016 (2016) 9174891.